The Los Alamos Sferic Array:
Ground truth for the FORTE satellite

D. A. Smith, K. B. Eack, J. Harlin, M. J. Heavner,
A. R. Jacobson, R. S. Massey, X. M. Shao, and K. C. Wiens

29 September 2000

NIS-1
Los Alamos National Laboratory
Los Alamos, NM 87544

Abstract

Operation of the Los Alamos Sferic Array (LASA) began in 1998 as an experimental system to study thunderstorms in support of FORTE satellite-based lightning research. The array started with five electric field change meters in New Mexico in 1998 and was expanded to eleven in New Mexico, Texas, Nebraska, and Florida in 1999. During the two years of operation described in this paper, the remote stations acquired triggered 8- to 16-millisecond duration, 12-bit sferic waveforms and GPS-based sferic time tags 24 hours per day year-round. Maps of source locations determined using differential time of arrival techniques were generated daily, and the waveforms from all geolocated events were transferred to Los Alamos National Laboratory (LANL) where they have been archived for further analysis including event classification and characterization. The array located nearly 1 million events during 1998 and 1999, of which over 2400 were tightly coincident (occurring within 300 μs, corrected for time of flight) with FORTE radio frequency triggers. The 2-D location uncertainty for events occurring within 130 km of the NM and FL sub-arrays was better than two kilometers, as determined through a comparison with data from the National Lightning Detection Network (NLDN). The purpose of this paper is to provide a description of the Los Alamos Sferic Array and to present initial results on the topics of event classification and comparative studies with FORTE and the NLDN.

1. Introduction

The Los Alamos Sferic Array (LASA) was developed to support lightning research in support of FORTE, the Fast On-orbit Recording of Transient Events satellite, which was launched into a 69-degree inclination, 800 km orbit in August of 1997. The purpose of FORTE has been to study transient VHF radio and optical emissions from the earth for the purpose of nuclear weapon monitoring research. Its primary research payloads include two twenty-MHz-bandwidth RF (radio frequency) receivers, a one hundred-MHz-bandwidth RF receiver, an optical imager, and an optical photodiode detector. These instruments regularly record the radio and optical emissions from terrestrial lightning discharges. FORTE RF payloads and observations have previously been described by *Massey et al.* [1998], *Jacobson et al.* [1999], *Jacobson et al.* [2000a], and *Suszcynsky et al.* [2000]. Optical payloads, observations, and modeling have been described by *Kirkland et al.* [1998], *Suszcynsky et al.* [1999], *Light et al.* [2000], *Suszcynsky et al.* [2000a], and *Suszcynsky et al.* [2000b].

A significant portion of the FORTE science effort has focused on the merging FORTE RF and optical observations with those from other satellite-based and ground-based resources. This data fusion has enhanced the value of FORTE observations in at least three respects: 1. Sensors with the ability to accurately geolocate sources have provided locations for events that FORTE has recorded but been unable to locate (FORTE's limited geolocation capabilities have been described by *Suszcynsky et al.* [2000b], *Jacobson et al.* [1999], and *Jacobson and Shao* [2000b]); 2. Multiple characterizations of the same stroke, flash, or storm using different sensor types have provided insight into thunderstorm electrification and discharge processes that no single sensor has been able to provide; 3. Sensors capable of continuously observing storms have provided a context for FORTE data collection, which is limited to the observation of a single point on the ground for only fifteen minutes (at most) per 100-minute orbit with no guarantee of revisiting the point on the subsequent orbit.

An example of a resource that has been used to supplement FORTE data analysis is the National Lightning Detection Network (NLDN), which has played a role in the processing of FORTE data acquired over North America. The NLDN provided locations, event identifications, and current estimates for nearly 15,000 FORTE-coincident events in 1998 [*Jacobson et al.*, 2000a] and over 10,000 in 1999 [*Jacobson*, private communication]. Other resources that have been utilized for FORTE comparative analyses include the Kennedy Space Center (KSC) Lightning Detection and Ranging (LDAR) system [*Lennon and Maier*, 1991], New Mexico Tech Lightning Mapping Array (LMA) [*Rison et al.*, 1999b], the Brazilian Lightning Detection Network (BLDN) [*Pinto et al.*, 1999], visible and IR space-based imagers (e.g. GOES), and the NEXRAD weather surveillance radar network.

The Los Alamos Sferic Array was developed as a resource to locate, classify, and characterize lightning discharges in support of FORTE. One advantage of operating our own ground-based array is that we have been able to tailor array operations for coordination with FORTE in order to maximize the likelihood of coincident observations. A second advantage has been our ability to retain all waveforms from all located events to permit detailed reanalysis of data. This brute-force approach to data archival has allowed us to evolve and optimize our processing techniques and apply them back to a very large collection of ground-based sferic and satellite-based RF waveforms. As we have advanced our understanding of lightning and developed new questions, the ability to reprocess these waveform data has been valuable, much more so than had we retained only waveform parameters. The array also has the potential to contribute to thunderstorm and lightning research independent of FORTE, and has already begun to do so.

Conceptually, LASA is an expansion of the 3-station array utilized by *Smith et al.* [1999a] (see also *Smith* [1998]) to make observations of compact intracloud discharges (CIDs) and other thunderstorm discharges in New Mexico and west Texas during the summer of 1996. The successes of both the previous array and the current array have been made possible by the marriage of a well-established sensor technology, the electric field change meter [*Krehbiel et al.*, 1979], with the modern-day capability to derive

accurate, absolute time tags at multiple, distant locations using GPS (Global Positioning System) receivers. The LANL sferic array has additionally made use of the internet to cost-effectively manage multiple, unattended sensors and to retrieve hundreds to thousands of Mbyte of waveform data on a daily basis.

This paper describes the operation and performance of the LANL sferic array, providing an overview of the first two years of operation and highlighting some initial results. The geolocation performance has been evaluated through a comparison with data from the NLDN. Among the initial results have been the development of an automatic identification scheme for finding CIDs in the LASA database and an evaluation of the success of joint LASA/FORTE observations in 1998 and 1999.

2. Instrumentation

2.1. Array Overview

We began operation of the Los Alamos Sferic Array with five stations (only four of which were independently located) in New Mexico in 1998. The stations were located in Los Alamos (two stations), Socorro, Roswell, and Tucumcari. In 1999 the array was expanded to eleven stations (all independently located) with four stations in New Mexico (in the previously mentioned locations); one in Omaha, Nebraska; one in Lubbock, Texas; and five in Florida in the following locations: Kennedy Space Center, Tampa, Fort Myers, Boca Raton, and Gainesville. Table 1 lists the station locations, 2-letter station identifiers, host facilities, and the starting and stopping (where applicable) dates of operation. Figure 1 is a map of the 1998 and 1999 LASA station locations.

As shown in Figure 1, the 1998 array consisted of a single cluster of stations that nearly formed a square with ~200 km separating the stations along the perimeter. The configuration was optimized for lightning studies in and near the state of New Mexico.

The 1999 array consisted of two 5-sensor station clusters, one in New Mexico/Texas (despite the station in Texas, the cluster will be referred to as the New Mexico array in this paper) and one in Florida, with an additional outlying station in Nebraska. The baselines for the NM and FL clusters, or sub-arrays, were on the order of 200 km. Utilizing the two-cluster array plus the additional station in NB, we were able to perform high sensitivity, high location accuracy studies within and near each sub-array, and were simultaneously able to detect and locate (with less accuracy) large-amplitude events that occurred over a large portion of the southern and central United States.

Except where footnoted in Table 1 and during temporary computer or network outages, LASA stations were operated twenty-four hours per day from their starting dates through the end of 1999 (and beyond, but this paper addresses only the 1998/1999 data).

The primary goal for 1998 was to support FORTE and gain experience in the remote operation of an array through the establishment of stations close to Los Alamos. The nearby locations simplified the deployment and servicing of the stations and also allowed us to make comparative observations with the New Mexico Tech LMA, which was operated in the vicinity of Socorro during the latter part of the 1998 thunderstorm season. *Rison et al.* [1999a and 1999b] have described joint LASA/LMA observations of narrow bipolar pulses (CID waveforms) that were made during this campaign.

The expansion to Florida in 1999 was motivated by the following factors: (1) the Florida peninsula features the highest flash density in the Unites States [*Cummins et al.*, 1998b]; (2) the location provided us with the opportunity to make thunderstorm observations in a maritime environment; (3) for operational reasons related to the locations of the FORTE ground stations (in Albuquerque, NM and Fairbanks, AK), the FORTE satellite was able to spend more time acquiring data over Florida than over New Mexico, increasing the likelihood of achieving LASA/FORTE coincidental detections; (4) the LDAR system at KSC, which produces accurate, highly-resolved, 3-D maps of lightning RF sources within ~100 km of km of Cape Canaveral [*Boccippio et al.*, 2000], is located on the perimeter of our Florida sferic array and is available for joint lightning studies.

The Omaha station was installed and made operational in 1998, but was not incorporated into daily LASA processing until 1999. It was originally deployed to support sprite research in the Great Plains region of the US, but has since proven to be useful for long-range studies of lightning discharges in general.

2.2. Station Description

The requirements for LASA site locations included a relatively quiet noise environment at VLF/LF radio frequencies, access to AC power and a high speed internet connection in close proximity to an outdoor rooftop location, and the existence of a cooperative host

institution and/or individual. Of these, the requirement for an internet connection generally presented the most serious restriction on potential sites.

Figure 2 is a block diagram of a LASA electric field change installation. All stations were identical in configuration except for the highpass and lowpass signal filters, which were added in 1999 and were not the same for all stations. Figure 3 is a photograph of the array station at the University of Florida in Gainesville. The 'inverted salad bowl' or 'hairdryer' design was adapted from M. Brook of New Mexico Tech and was previously described by *Smith et al.* [1999a]. The stainless steel dome suspended from the 'neck' of the field change meter in the figure shields a 38 cm diameter sensing plate from precipitation, which can cause spurious field change signals at the meter output as a result of charged raindrops. A charge amplification circuit inside the dome was fed from the sensing plate and configured with a 1-ms decay time constant. A 50 Ω line driver sent the field change output signal through 30 m (typically) of coaxial cable to the interior of the building. Rising from the neck of the field change meter in Figure 3 is the GPS antenna/receiver for the station. It connects to a card in the computer inside the building and provides absolute (UTC) event time tagging with an accuracy of better than 2 μs.

As mentioned earlier, the lowpass and highpass filters were added in 1999. The lowpass filters had a cutoff frequency of 500 kHz and were inserted to prevent aliasing by the 1 Msamp/s waveform digitizer. We had previously concluded that the anti-aliasing filters were not necessary due to a roll-off in the field change meter frequency response above the Nyquist sampling frequency. However, at two of the stations, the roll-offs were not steep enough to prevent transmissions from powerful, local AM radio stations (with center frequencies near 1 MHz) from aliasing into the digitized sferic waveforms. The lowpass filters eliminated the interference problem. The highpass filters were added in 1999 to eliminate DC offsets in the outputs at some of the Florida stations (possibly caused by leakage current due to high humidity), and also to address a 60 Hz noise problem at the Fort Myers station. The 3 dB cutoff frequencies at all stations except Fort Myers (FM) were 34 Hz. The FM cutoff was 340 Hz. The difference is noticeable in

waveforms or waveform segments dominated by low frequency signal components, when the FM waveforms are more severely attenuated.

The filtered field change signal was split between a 12-bit analog-to-digital converter (A/D) card in the computer and an external trigger module, which was used to implement trigger criteria. The trigger module accepted positive and negative DC thresholds from a digital-to-analog converter (D/A) card in the computer. The two thresholds were separately and remotely adjustable and were used to define the thresholds at which the bipolar trigger circuit would trigger data acquisition. During 1998 the thresholds were adjusted infrequently and simply left at a threshold that produced a comfortable trigger rate. During 1999, a 'campaign mode' of operation was implemented to maximize the likelihood of making coincident observations of FORTE-detected events and to also study long-distance sferic propagation. In campaign mode, monthly schedules of threshold changes were sent to the remote stations where resident scheduling programs raised and lowered station thresholds in conjunction with FORTE passes and at other regular time intervals when increased sensitivities were desired. Typical thresholds during campaign mode and non-campaign mode were ±1.5 V/m and ±6 V/m respectively. As described in more detail later, campaign mode increased the likelihood of a given array event being detected by FORTE by a factor of four from 0.074% in 1998 to 0.30% in 1999. Figure 4 provides an example of the increased sensitivity at the LA array station during campaign mode segments on 07-09-1999. The graph shows trigger rate (triggers per minute) as a function of time of day (UTC) with periods of high sensitivity indicated by horizontal bars at the top of the graph. The brief (5- to 15- minute duration) increases in trigger rate correspond to periods of lowered thresholds and result from weaker and/or more distant lightning activity. Plots like Figure 4 were automatically generated daily and made available over the World Wide Web as part of array state-of-health monitoring.

Trigger signals from the trigger module were sent to the A/D and GPS cards in the computer, which recorded field change waveforms and time stamps with each trigger. With the exception of the LO station, all stations acquired 8 ms waveforms sampled at 1 Msamp/s during 1998 and 1999. The pretrigger fractions for non-LO stations in 1998

and 1999 were 50% and 25% respectively. The LO station was operated in 1998 only and acquired 1 Msamp/s, 16 ms duration records with 25% pretrigger. The motivation behind the LO station configuration was to look for sprite signatures in the tails of positive cloud-to-ground (CG) lightning stroke waveforms. The dead time between triggers for the individual stations during 1998 ranged from 30 to over 100 milliseconds, depending on the time required to write each waveform to disk. This time was found to be a function of the fullness of the data directory. For 1999 the data directory structures of the stations were modified to reduce the dead time between triggers, so that the re-trigger time was consistently less than 40 ms. Reducing the dead time increased the likelihood of detecting subsequent CG return strokes.

Each time a trigger was produced by a remote station, the sferic waveform was written to a binary file, and the UTC time tag (from the GPS receiver) was written to a separate header file, which was used to log daily station time tags. Waveform filenames included the year, month, day, station identifier, and event number. Data acquisition proceeded in this fashion until the UTC day rollover, when data acquisition was automatically restarted to allow transfer and processing of the previous day's data. As part of the restart, the header file from the previous day was closed, and the waveform filenames were updated to reflect the new date.

An event rate limiter was implemented in software at each remote station to prevent the hard drive from filling up in the event of an extremely high trigger rate resulting from a close lightning storm or the appearance of a new or intermittent noise source. During times when the rate limiter was activated, waveform acquisition halted but time tag acquisition continued.

In order to minimize the time and effort required to monitor the state of health of the array, each station was programmed to send a daily status report by electronic mail to the LANL operators. The email messages reported the number of waveforms acquired during the day, the remaining capacity of the station data hard drive, the time of the last waveform of the day (used to determine whether the software was running through the

day rollover), and any problems encountered during the day (whether the rate limiter was engaged) . The messages eliminated the need to log onto each station each day to determine its status.

During 1998 and 1999 the field change hardware, computers, operating systems, and software functioned reliably. In part due to this reliability and in part due to the cooperation of our colleagues at the remote sites, it was not necessary for LANL personnel to visit the stations at any time for troubleshooting following initial station operating capability.

2.3. Array Processing

Like the remote stations, the LANL array processing computer (APC) operated automatically (without operator intervention) on a daily cycle. The first task following the UT day rollover was to transfer (via the internet) the previous day's header files from the remote stations to LANL, where temporal coincidences involving a minimum of three stations were identified (three stations are required to make a 2-D source location determination). The width of the coincidence time window was determined by the time required for a radio signal to transit (at the speed of light) the longest chord of the array, since this time represents the largest possible differential time of arrival (DTOA) for a real event. A slightly longer window was implemented in practice to allow for the possibility that stations trigger on the same event, but not on the same waveform feature. In 1998 the window was 2 ms, corresponding to the delay between the RO and LA stations. In 1999 the window for the complete eleven-station array was 10 ms, corresponding to the delay between the BR and LA stations.

Having identified the temporal coincidences between array stations, the APC would direct the remote computers to compress the coincident waveforms for subsequent retrieval and decompression. Following the retrieval of all data for the day, waveforms were cross-correlated to determine timing corrections between the events recorded by different stations. In addition to making fine timing corrections, this step was used to

reject (on the basis of poor cross correlation coefficients) waveforms suspected to originate from different sources. Different sources may refer to a source of noise that affects one station or may refer to two separate lightning flashes that occur at nearly the same time (within milliseconds of each other) at different locations. Figure 5 shows an example of multiple waveforms recorded from a single positive CG flash that occurred in the Texas Panhandle in Mid-May of 1999. The waveforms were recorded by the LB, TU, RO, and SO stations from ranges of 101, 291, 344, and 554 km respectively. The flash was characterized by NLDN as a +CG with a peak current of 101 kA. Note the polarity convention used throughout this paper, that initially-positive radiation field waveforms indicate current flow from above to below. The figure shows more pronounced ionospheric effects with increasing distance from the source. The negative excursion in the SO (bottom) waveform occurs at the expected single-hop ionospheric delay time given the source range (554 km) and an ionospheric virtual reflection height of 70 km (typical for the late-afternoon, which is when this flash occurred).

Cross correlations were not performed on the entire sferic waveforms. This was found to be burdensome with regard to computational intensity and also produced occasional bogus cross correlations as a result of ionospheric reflections or noise. Because most sferic waveforms have a single, prominent feature that lasts much less than one millisecond, correlations were performed on 512 point (512 μs) windows centered on the peak absolute waveform amplitudes. Care was taken to assure that the peaks from different waveforms corresponded to consistent polarities, in case the positive and negative peak amplitudes were similar.

The cross correlation coefficients for the waveforms in Figure 5 are 0.95, 1.00, 0.97, and 0.85 respectively. As indicated by the unity coefficient for the second waveform, the cross correlations were performed with respect to the second waveform in time order of arrival. This has been the standard convention for LASA waveform correlation because it guarantees that the template waveform is dominated by the radiation component of the electromagnetic field, and not by the intermediate or static components, which can

seriously alter the field change wave shape within several tens of kilometers of a recording station.

Figure 6 shows waveforms recorded from a negative CG (59 kA peak current as reported by the NLDN) that occurred 25 km southwest of Los Alamos and was recorded by the LA, TU, and LB stations. The Los Alamos (top) waveform features a large negative DC offset at time zero that saturated the meter. This is the static component of the field radiated by the return stroke. The exponential decay following the stroke is a characteristic of the field change meter electronics that allows subsequent strokes or flashes to utilize the same instrumental dynamic range by returning the trace to zero within a few milliseconds. The radiation field from the stroke is superimposed on the decaying exponential. By always performing the cross correlations with respect to the second waveform (except for 1998 cases when the first two stations were the co-located LA and LO sensors, in which case we used the third waveform as the template), it is guaranteed that the template waveform is always recorded from a distance of at least half the length of the shortest array baseline or approximately 80 km. Although this convention assures the choice of a reasonable template, it does not address the poor correlations that can result when the first waveform is close to the source. The correlation coefficients for the waveforms in Figure 6 were 0.58, 1.00, and 0.80. The poor (but not awful) correlation between the first two waveforms results largely from the static component of the LA waveform. As waveforms differ from each other to a greater extent, the time lag adjustments are affected more adversely, which ultimately affects the accuracy of the location solution. The LASA event location for the Figure 6 negative CG differed from the NLDN location by 2.6 km, whereas the typical difference for events that close to an array cluster is less than 1.5 km (as will be shown later). The NLDN addresses the problems associated with static radiation by not using stations within ~50 km of an event to assist in the source location determination. This is an appropriate solution for a well-populated and large array, but would lead to the elimination of too many waveforms with our array. The inclusion of static waveforms may adversely affect the overall location accuracy of LASA, as mentioned later in this paper.

It was stated earlier that correlation coefficients are used to eliminate very poor waveform matches. The minimum coefficient for first waveforms is 0.20. The minimum for third, fourth, etc. waveforms is 0.55. It is not unusual for waveforms with a significant static component to be rejected on the basis of this criterion. When this occurs and the total number of contributing stations is greater than three, the location solution is derived from the remaining stations. When the number of contributing stations is equal to three, then the event is rejected because three stations are required to locate an event. A final interesting note on Figure 6 is that both static and radiation (and/or intermediate) field terms are observable in the approaching leader prior to the attachment near time zero.

Following waveform cross correlation, the APC determines event locations using the correlation-adjusted DTOAs. The location solution is determined using a multidimensional downhill simplex method [*Nelder and Mead*, 1965] called Amoeba [*Press et al.*, 1986]. Similar sferic location methods have been described and employed by *Lee* [1989]. Prior to running the location algorithm, the software verifies that the inter-station DTOAs are physically possible, i.e. less than the inter-station speed-of-light propagation times. Stations with times that do not meet this criterion are rejected from the solution determination. Additionally, three-station events that include both LA and LO (the co-located sensors) are rejected from the database because there exists only one independent DTOA each of for these events.

Figure 7 shows a map of event locations in the vicinity of the NM array on 04-30-1999. All events recorded by at least three stations are pictures, with the total event count being greater than 10,000. Colored diamonds are used to indicate event location as a function of time of day (UT) with dark blue corresponding to 1800 local time on 04-29 and red corresponding to the same time on the following day. The NM array station locations are represented by black circles connected by black lines. From the map, it is discernable that the lightning was associated with frontal activity since the event rate is more or less constant throughout the day, the activity shows general motion from the northwest, and the events occur in lines that are generally perpendicular to the direction of storm motion.

Airmass thunderstorms, which typically become active later in the spring or summer, generally do not continue to produce intense activity through the late night and into the following morning. The map is a nice example of activity occurring in the vicinity of an array cluster. Campaign mode was active throughout the day, so station thresholds varied between ~2 V/m and ~6 V/m. Some of the color banding that is evident is likely due to the threshold variations during FORTE overpasses.

Figure 8 shows a map of event locations from a different day on a much larger scale. The four (or so) wintertime storms pictured occurred on 12-12-1999 when the thresholds at all stations were left unusually low (0.5 to 1.5 V/m for most stations) for the entire day (no campaign mode). A large frontal thunderstorm system can be seen moving from Texas through the South. Another large system at a range of over 1500 km from any array stations was active in the Atlantic Ocean. A couple of additional systems are visible in the Caribbean Sea. The location accuracies for such distant storms are discussed later in this paper. Events that occurred in the system over the U. S. were certainly located with more accuracy than events occurring outside of the array, since they were observed with much better viewing geometry. Evidence of this is shown by the uniform color variations in the Texas/Louisiana storm compared to the off-shore storms. Maps similar to those pictured in Figures 7 and 8 were generated automatically every day and made available over the internet to assist in array state-of-health monitoring.

Station ID	Initial Operation Date	Location	Host Facility
LA	04-06-1998	Los Alamos, NM	LANL
SO	05-01-1998	Socorro, NM	New Mexico Tech
RO	05-12-1998	Roswell, NM	Eastern New Mexico University
TU	05-27-1998	Tucumcari, NM	Mesa Technical College
LO*	07-01-1998*	Los Alamos, NM	LANL
CR	02-09-1999	Omaha, NE	Creighton University
KC	04-05-1999	Cape Canaveral	Kennedy Space Center
TA	04-06-1999	Tampa, FL	University of South Florida
FM	04-08-1999	Fort Myers, FL	Cyberstreet ISP
BR	04-08-1999	Boca Raton, FL	Florida Atlantic University
GV	04-09-1999	Gainesville, FL	University of Florida
LB	04-27-1999	Lubbock, TX	Texas Tech University

*The LO station was the second of two stations in Los Alamos during 1998. It was decommissioned on 08-11-1998

Table 1. List of Los Alamos Sferic Array stations, locations, and dates of operation.

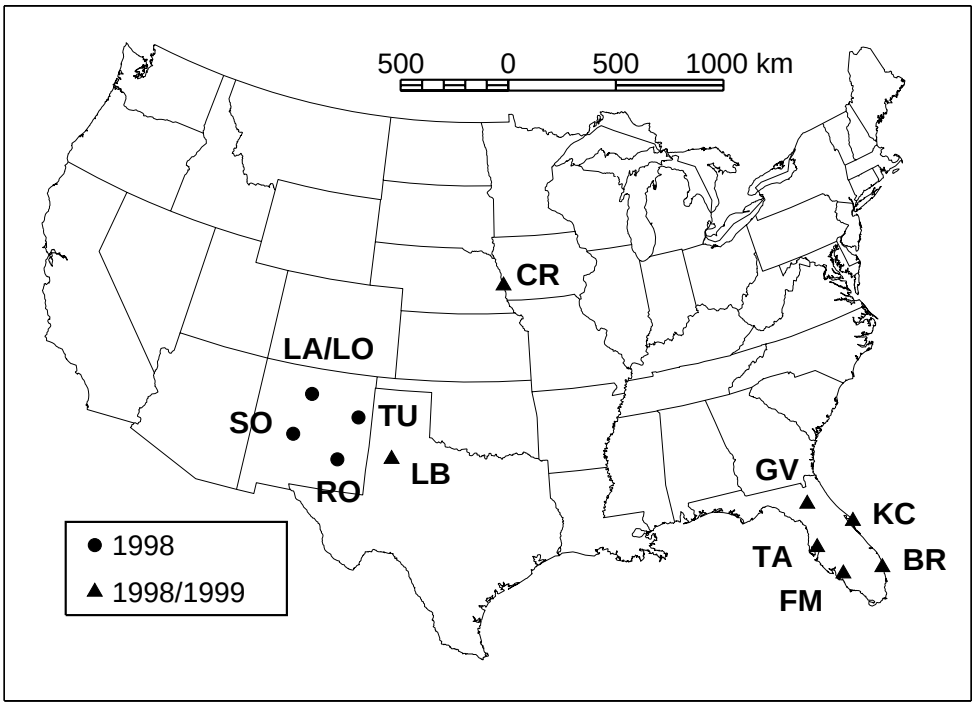

Figure 1. Map showing the locations of the 1998 and 1999 Los Alamos Sferic Array stations.

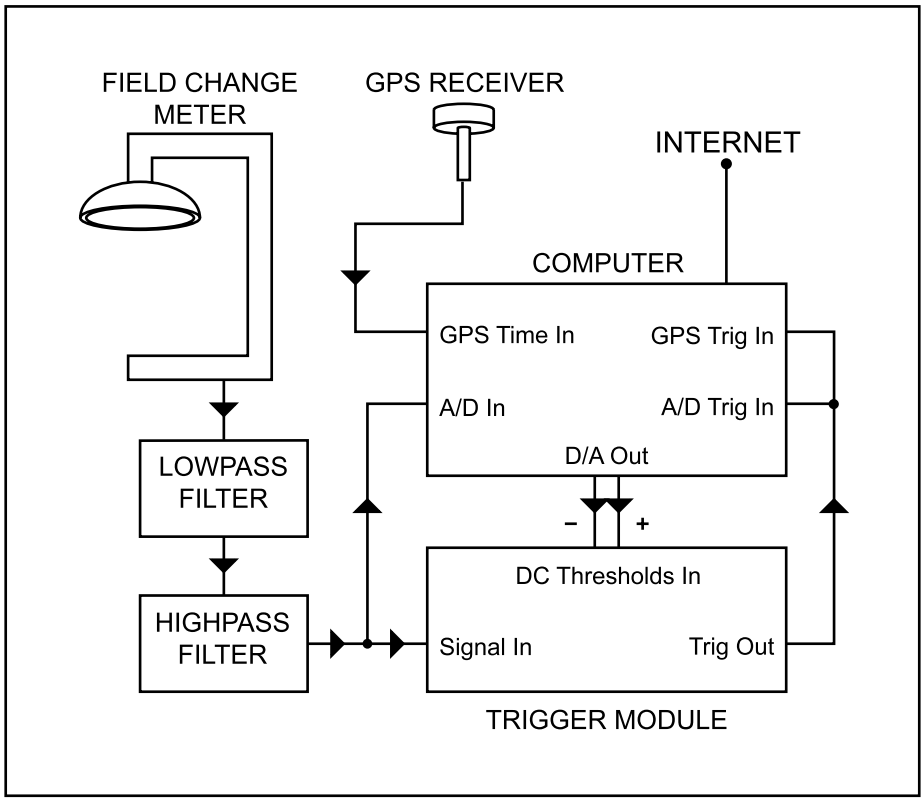

Figure 2. Block diagram of a Los Alamos Sferic Array station.

Figure 3. Photograph of the sferic array station at the University of Florida in Gainesville.

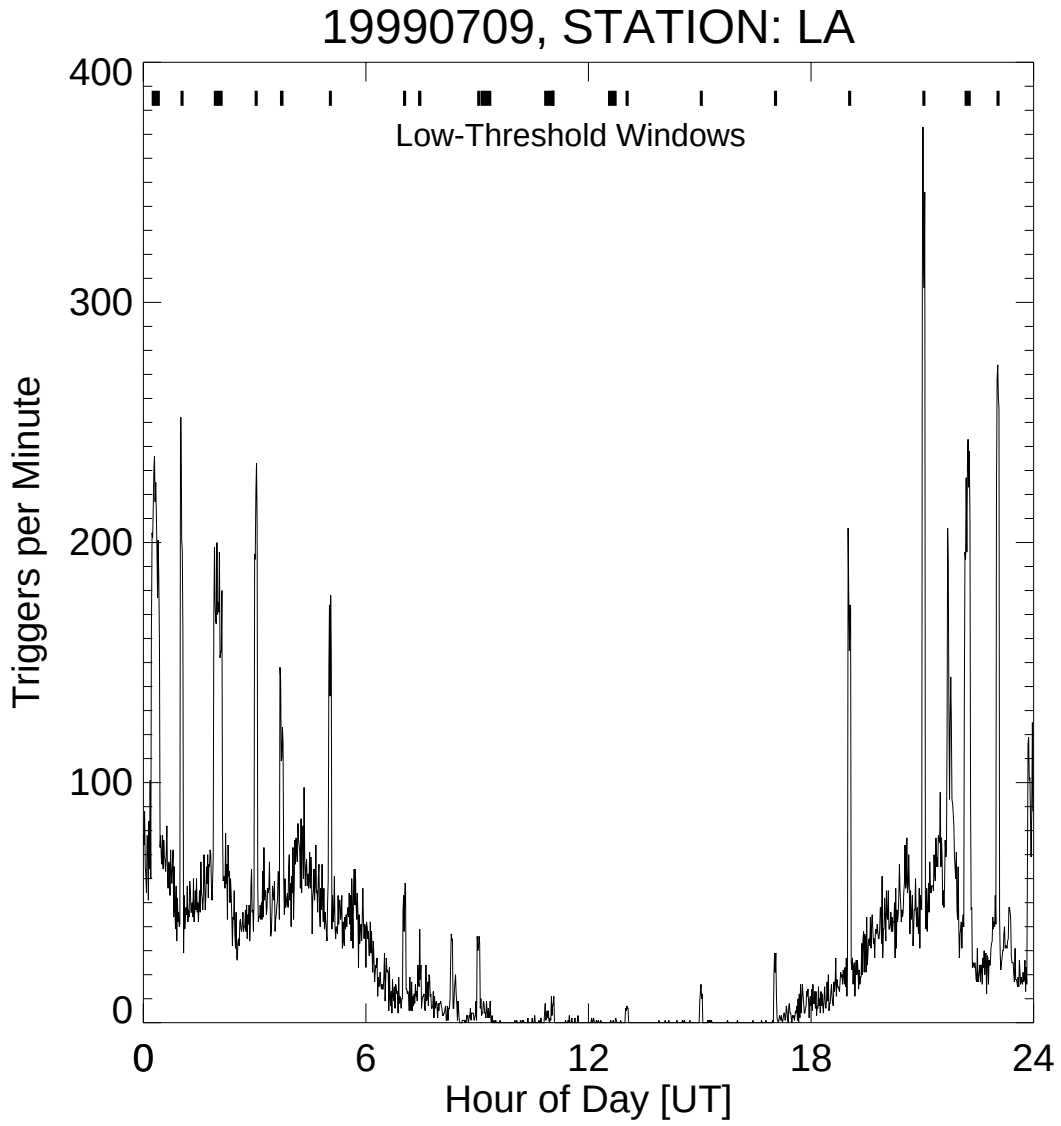

Figure 4. Plot of the trigger rate as a function of time for the Los Alamos array station on 07-09-1999. Bars along the top of the figure indicate low threshold time periods associated with 'campaign mode.'

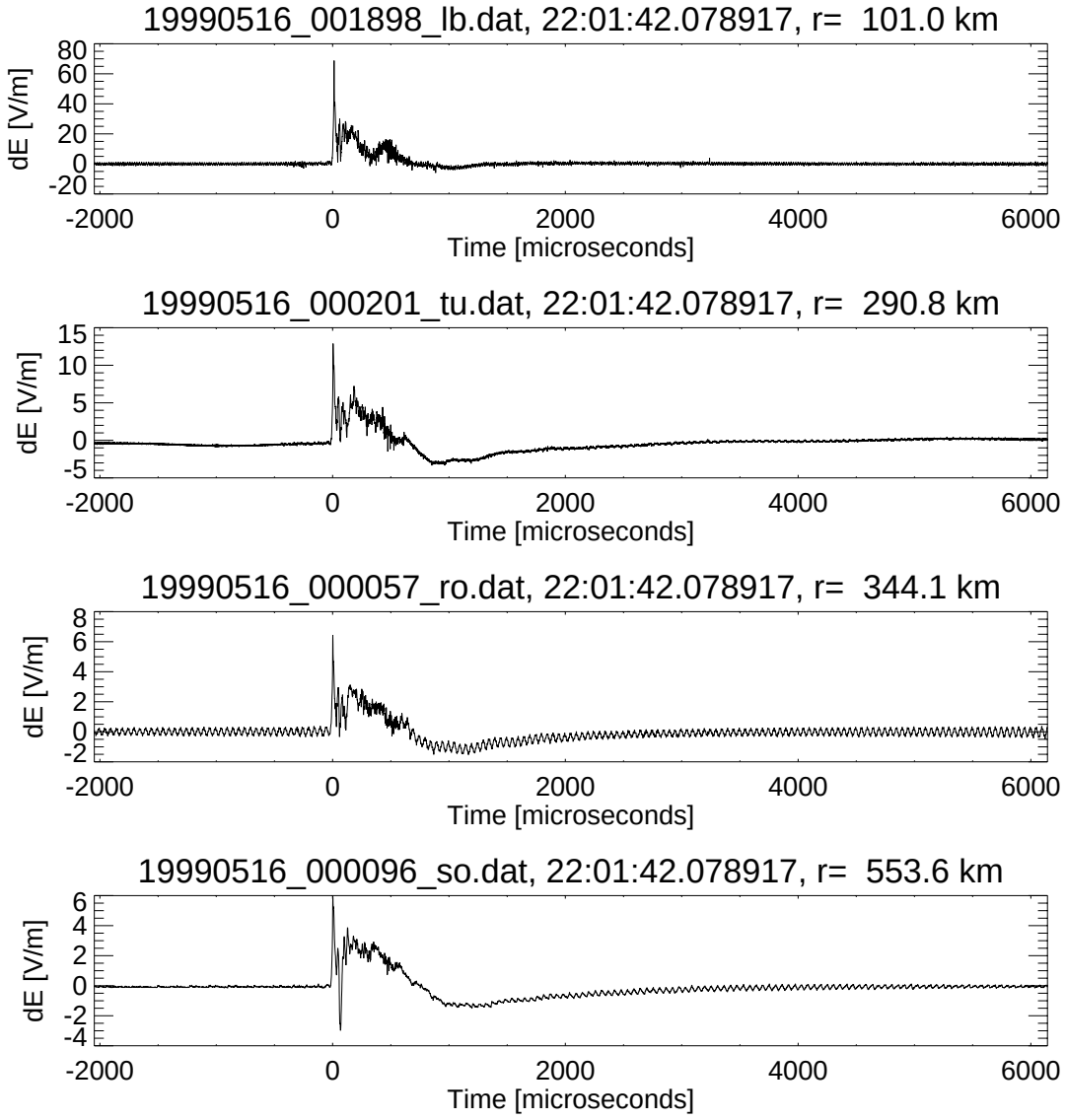

Figure 5. Field change waveforms from a positive cloud-to-ground lightning return stroke that occurred in the Texas Panhandle.

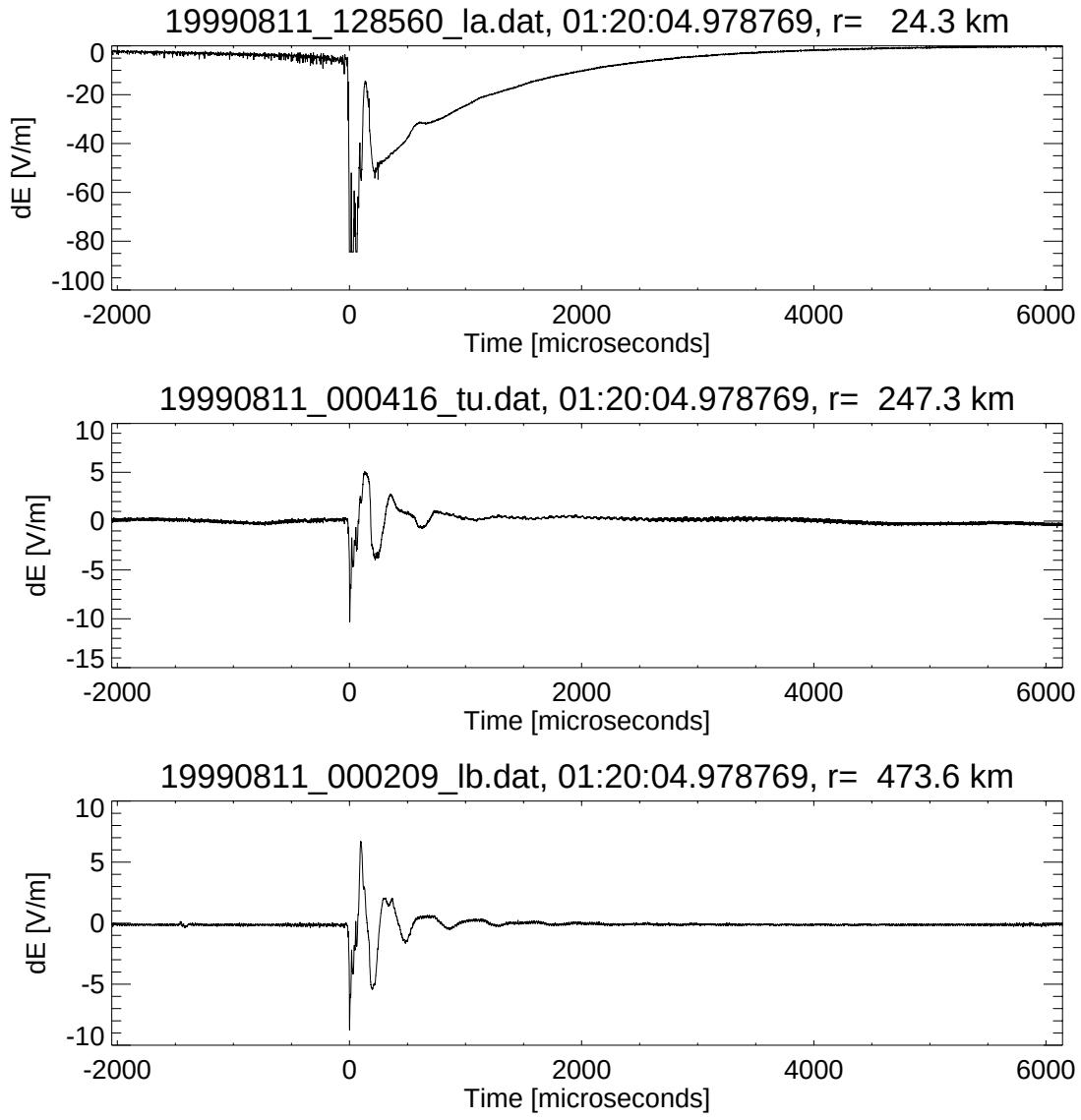

Figure 6. Field change waveforms from a negative cloud-to-ground lightning return stroke that occurred 24 km southwest of Los Alamos. The first waveform features a large static field component.

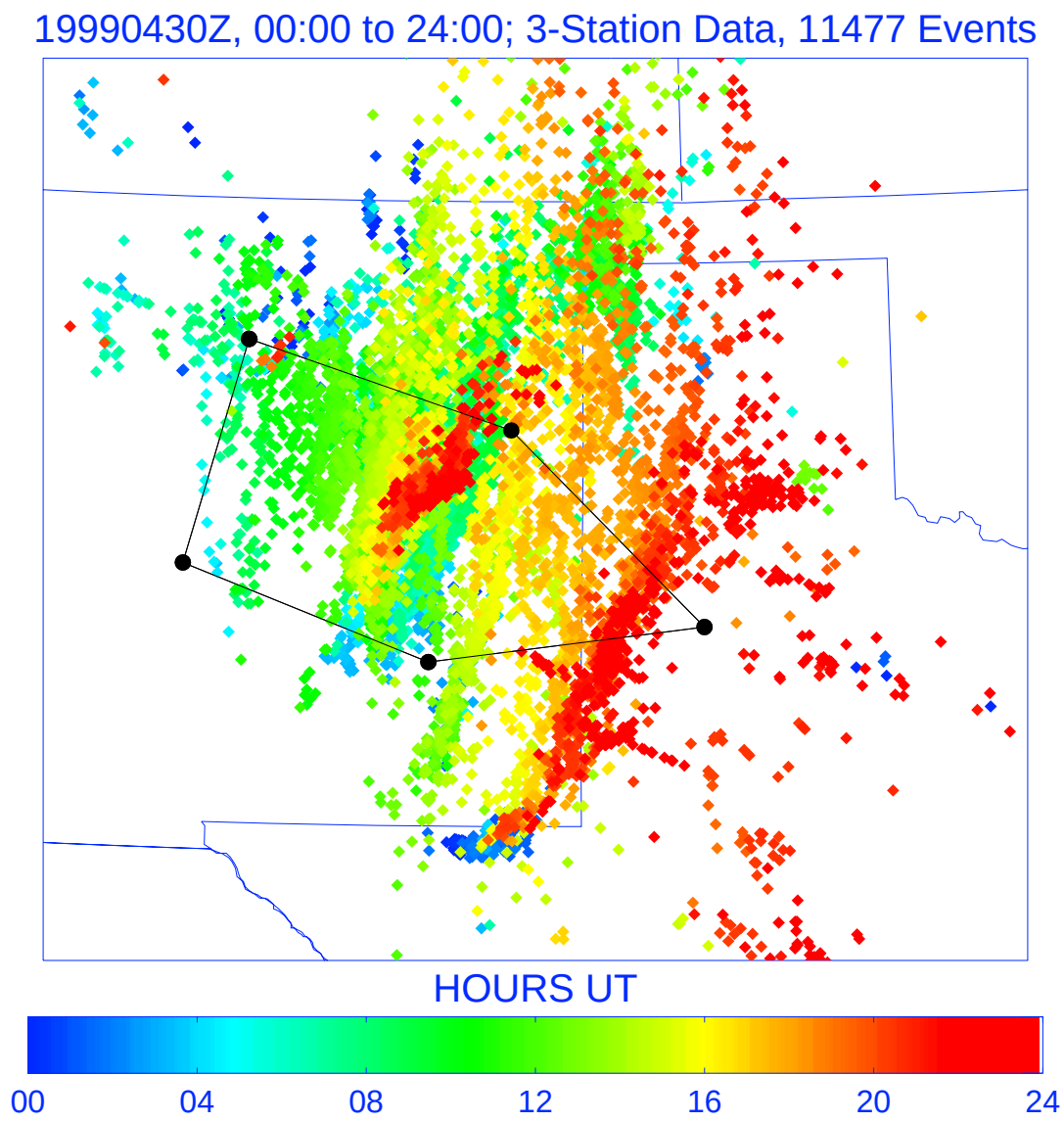

Figure 7. Map of array activity on 04-30-1999. Color indicates time of day (UTC).

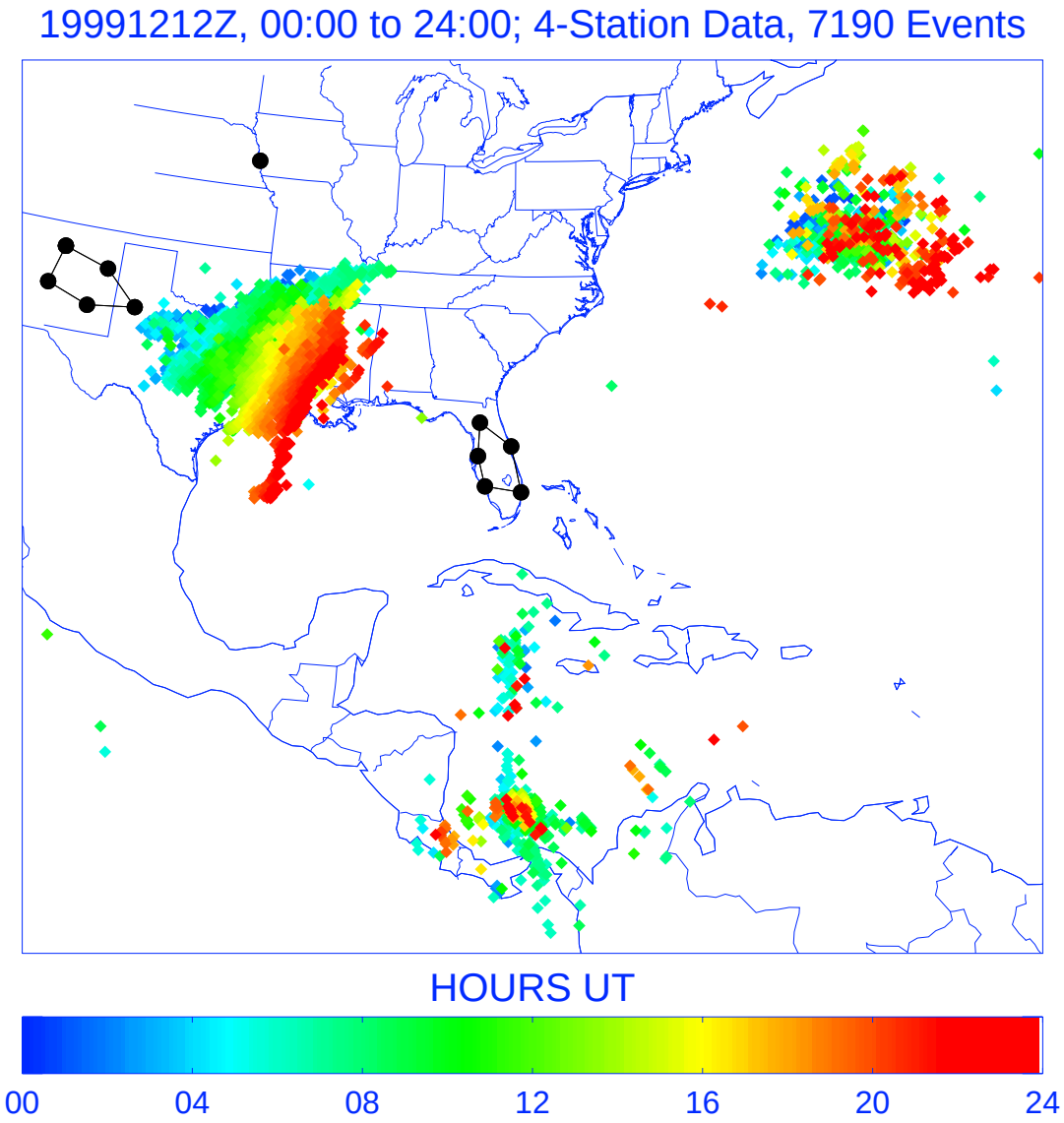

Figure 8. Map of array activity on 12-12-1999. Color indicates time of day (UTC). The map demonstrates the long-range capabilities of the sferic array.

3. Array Geolocation Accuracy

Time-of-arrival lightning location systems, using both low-frequency and high-frequency detection systems, have been described and utilized by many researchers including *Proctor* [1971], *Lennon and Maier* [1991], *Cummins et al.* [1998a], *Smith et al.* [1999a], and *Rison et al.* [1999b]. Limits on the accuracy and precision of such systems depend fundamentally upon the accuracy and precision of the absolute timing source or sources that are used to time tag events at each station. Further limits are imposed by unfavorable source viewing geometries or by the inability to adequately correlate waveforms received by multiple sensors.

Prior to the deployment of the Los Alamos Sferic Array, seven of the eleven GPS receivers were tested to characterize their absolute timing accuracies with respect to each other and with respect to a reference GPS receiver with an absolute accuracy of better than 100 ns. In our tests, the standard deviation of the timing difference between the reference receiver and a LASA receiver was less than 2 μs when periodic trigger signals were fed to the receivers over a period of several days. In similar tests conducted using the seven identical LASA receivers, the standard deviation of their timing differences was also less than 2 μs. It was concluded that we could reasonably expect absolute timing accuracy at each station that was accurate to within 2 μs of UTC. The receivers report time with a precision of 100 ns, however our measurements indicated that we could not expect comparable accuracy.

With favorable viewing geometry and perfect waveform correlation capability, the location accuracy of a TOA system should be comparable to the product of the timing uncertainty and the signal propagation speed (basically that of light for radio wave propagation in the atmosphere). Using this relationship, our 2 μs timing uncertainty corresponds to a location uncertainty of 600 meters. This was thought to be the best location accuracy that could possibly be expected from LASA.

3.1. LASA/NLDN Location Comparison

To evaluate the location accuracy of the Sferic Array we compared LASA event locations to lightning locations determined by the National Lightning Detection Network (NLDN) for six months (April through September) in 1998 and six months (May through October) in 1999. The NLDN data sets used for the comparisons were not standard NLDN data products, but were reprocessed from raw data using relaxed event criteria in order to maximize the detection of both intracloud discharges and distant/weak cloud-to-ground discharges. The 1999 data were processed with somewhat more strict criteria than the 1998 data. The standard NLDN data provide 80-90% detection efficiency of cloud-to-ground strokes with currents of greater than 5 kA within the limits of the conterminous United States (CONUS). These events are located with an accuracy of 500 m [*Cummins et al.*, 1998a]. The 'loosened criteria' data used for comparison in this paper may not meet these quality-control criteria. Their uncertainty has not been characterized.

The comparison was begun by identifying all 1998 and 1999 temporal coincidences between the two data sets within a ±20 ms window. A histogram of the resulting time differences is shown in Figure 9 with a bin size of 0.5 ms. A significant peak is present at zero lag. Before taking a closer look at the coincidence peak, it is worth noting the following facts: The 1998 and 1999 NLDN data sets often include over one million events per day during the summer months. One million events per day corresponds to twelve events per second or one every 80 ms. Furthermore, a coincidence window of 20 ms permits the inclusion of events separated by as far as 6000 km (20 ms times the speed of light). A six thousand kilometer diameter is large enough to cover all of CONUS, and thus includes the vast majority of NLDN events in the 1998 and 1999 databases (not necessarily all because some of the loosened criteria events were located far off-shore). The high event rate and large coincidence window mean that a large fraction of the events in the top panel of Figure 9 were simply coincidental detections of different events. In fact with an average inter-event time of 80 ms and a ±20 ms coincidence window, there is a 50% chance that a randomly selected time will have an NLDN coincidence on a busy (~1 million events) day for the NLDN. This is evidenced by the

fact that the area under the 'noise floor' in Figure 9 is comparable to the area under the correlation peak.

Figure 10 shows the LASA/NLDN time coincidence histogram over a range of ±1 ms with a bin size of 10 μs. The peak is well defined, with a half width of 7 μs (determined separately with finer binning) and a higher signal-to-noise ratio than the histogram from the previous figure. There exists a slight asymmetry in the peak in the form of a minor bulge on the right side of the peak. The bulge is indicative of a population of LASA events that occurred a few tens to hundreds of microseconds after their corresponding NLDN events. The asymmetry is attributable to the fact that NLDN utilizes a waveform extrapolation to zero amplitude to attempt to tag the attachment process (or, presumably, the first detected current rise for an intracloud stroke in the loosened criteria database). The LASA convention is to time tag the peak recorded electric field amplitude, which physically corresponds to peak *di/dt*. Slow rising LASA waveforms that do not peak until several tens to hundreds of microseconds after their initial rise cause the slight bulge visible on the right side of Figure 10. Not visible in Figure 10, but apparent on closer inspection with finer binning is that the histogram peak occurs at +2 μs, indicating that NLDN most often leads LASA by 2 μs in the time tagging of lightning discharges. Again this is consistent with the different time tag conventions.

Based on Figure 10, the time coincidence window for the location analysis was selected to be ±100 μs. The number of events within this window was 497,288. The number within the original ±20 ms window was 813,064. Figure 11 shows the cumulative log distribution of spatial separations between the LASA and NLDN event locations for events within the ±100 μs coincidence window for 1998-only and for the combined 1998/1999 databases. The bin size is 1.0 km. The figure shows that for the entire 1998/1999 database, 38% of the LASA/NLDN temporal coincidences agree to within 1 km, 85% to within 10 km, 99% to within 40 km, and 99.9% to within 220 km. Further analysis will address only the 1998 data because of the simpler array geometry (the stations very nearly formed a square as seen in Figures 1 and 7). The results for the 1998-only database were that 45% of the coincidences agree to within 1 km, 88% to

within 10 km, 99% to within 40 km, and 99.9% to within 220 km. From these data alone it does not appear that LASA even approaches the theoretical best location accuracy of 600 m.

Figure 12 shows the cumulative log distribution of 1998 LASA event ranges from the centroid of the 1998 New Mexico array (for events within ±100 μs of NLDN events). The previous figure showed that 88% of the 1998 event locations agreed with NLDN to within 10 km. Figure 12 shows that 88% of the LASA events occurred within 330 km of the centroid of the array, the suggestion being that that events within and close to the NM array may have been located with relatively good accuracy and that events occurring far away were not.

Location accuracy on an event-by-event bases is addressed in Figure 13, which is a log-log plot of the average LASA/NLDN location difference as a function of range from the NM array centroid. The figure shows that on average the event locations agree to within 1.3 km out to a distance of 70 km from the center of the NM array. They agree to within 2.0 km out to a distance of 130 km, a range that corresponds well to the edge of the NM array. Beyond this distance the location difference decays somewhat linearly to a range of 1000 km where the mean LASA/NLDN location difference is 25 km.

Earlier in this section it was asserted that 600 m location accuracy might be achievable under conditions of favorable geometry and assuming an excellent waveform cross correlation capability. Favorable geometry for the 1998 New Mexico array can basically be considered to exist within its perimeter. This is true intuitively and is backed up by the results illustrated in Figure 13. There are a few reasons that may explain why an agreement of 600 m was not achieved. The first is the fact that the NLDN lightning locations do not necessarily represent the true source locations. The uncertainty for the standard NLDN data product is 0.5 km. It is not known whether this accuracy is achieved for the region of New Mexico that includes the 1998 LASA stations . The effect of NLDN ‘loosened criteria’ (explained earlier) is also not known. From these observations we conclude that the NLDN accuracy is probably not better than 0.5 km. A

second consideration is that LASA waveform cross correlations are not perfect. With identical waveforms at all stations it would be possible to determine the actual DTOAs to within 1 μs; however the waveforms are not identical. Propagation over the finitely conducting ground, ionospheric reflections, and static-near and inductive-intermediate field influences all affect the wave shapes. It was hypothesized in the discussion of the Figure 6 waveforms that the 2.7 km difference between the LASA and NLDN locations resulted in part from the static contribution evident in the first waveform. A third consideration is the potential for contamination from incidental coincidences. The events used for this comparative study were selected by finding ±100 μs LASA/NLDN coincidences. Event ranges from the NM array centroid were based on the LASA event locations. Incidental NLDN events that occurred simultaneously (or nearly so) with LASA events, but occurred at great distances could be included in Figure 13. These events are relatively less likely to contaminate the close event range bins than the more distant ones due to effective spatial and temporal filtering, but the events certainly play a role in the Figure 13 plot beyond several hundred km in range.

The conclusion with regard to LASA event location accuracy is that events occurring within the NM and FL sub-arrays are well-located with an uncertainty of less than 2 km. The Florida result was not proven, but the argument is made based on the similar (or even shorter) baselines and the better propagation conditions in Florida. Also, both arrays certainly benefited from having five stations in 1999. Within an array diameter of each sub-array, it appears to be reasonable to expect location accuracy on the order of or better than 10 km. Beyond this distance, the accuracies degrade steadily with distance when the members of the sub-array are the only participants in the location determination. Not addressed in this analysis were events detected by members of more than one sub-array and/or by the satellite Omaha station. Having very distant stations participate in determining the location solution can be extremely useful in reducing errors, especially when the events being located lie close to the line joining the detecting stations. This is because it is the radial component of the uncertainty ellipse that rapidly elongates with distance away from a sub-array. Constraining the ellipse with a distant observation is effective at reducing the location uncertainty.

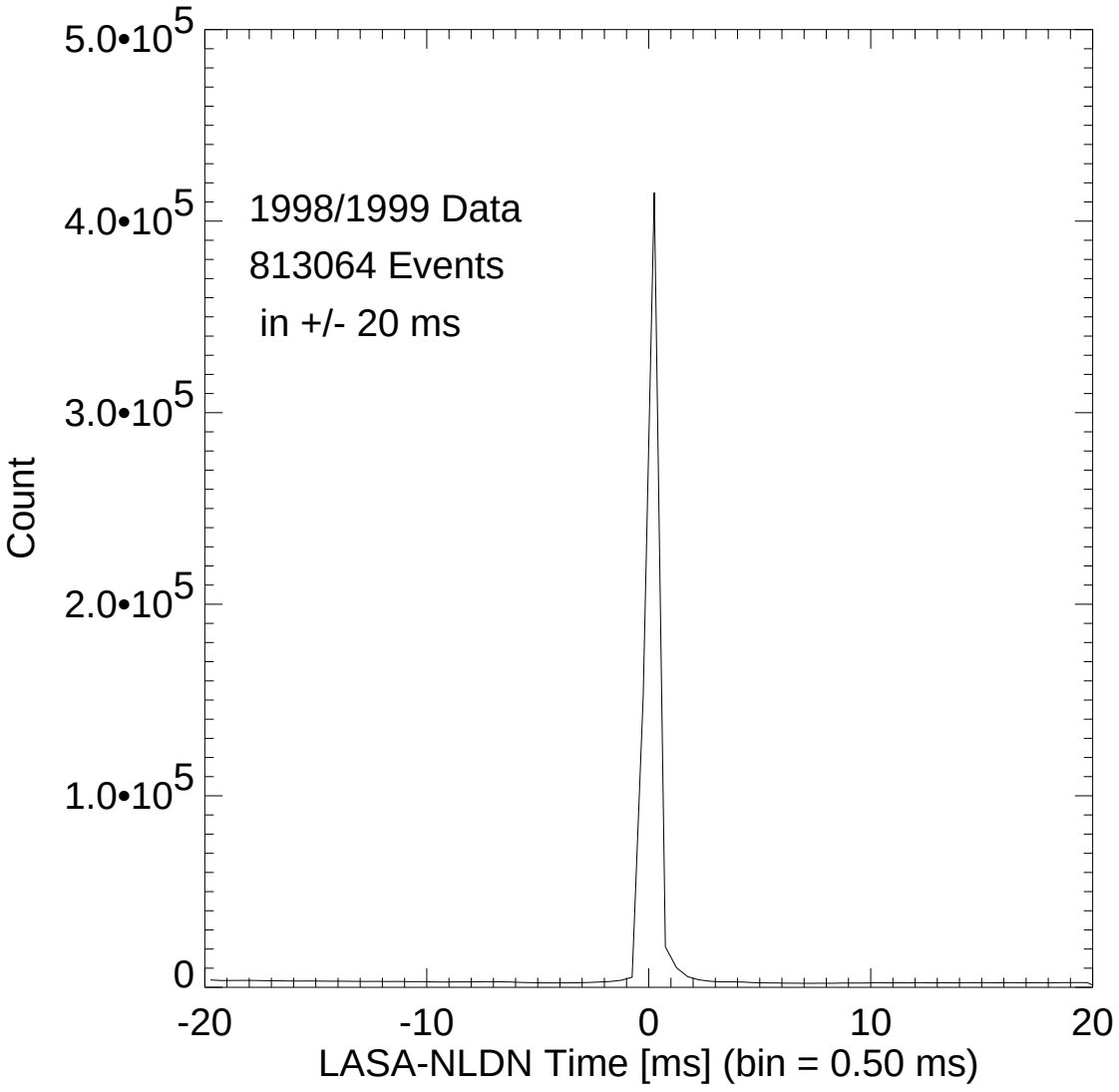

Figure 9. Histogram of LASA/NLDN time differences (1998/1999 data).

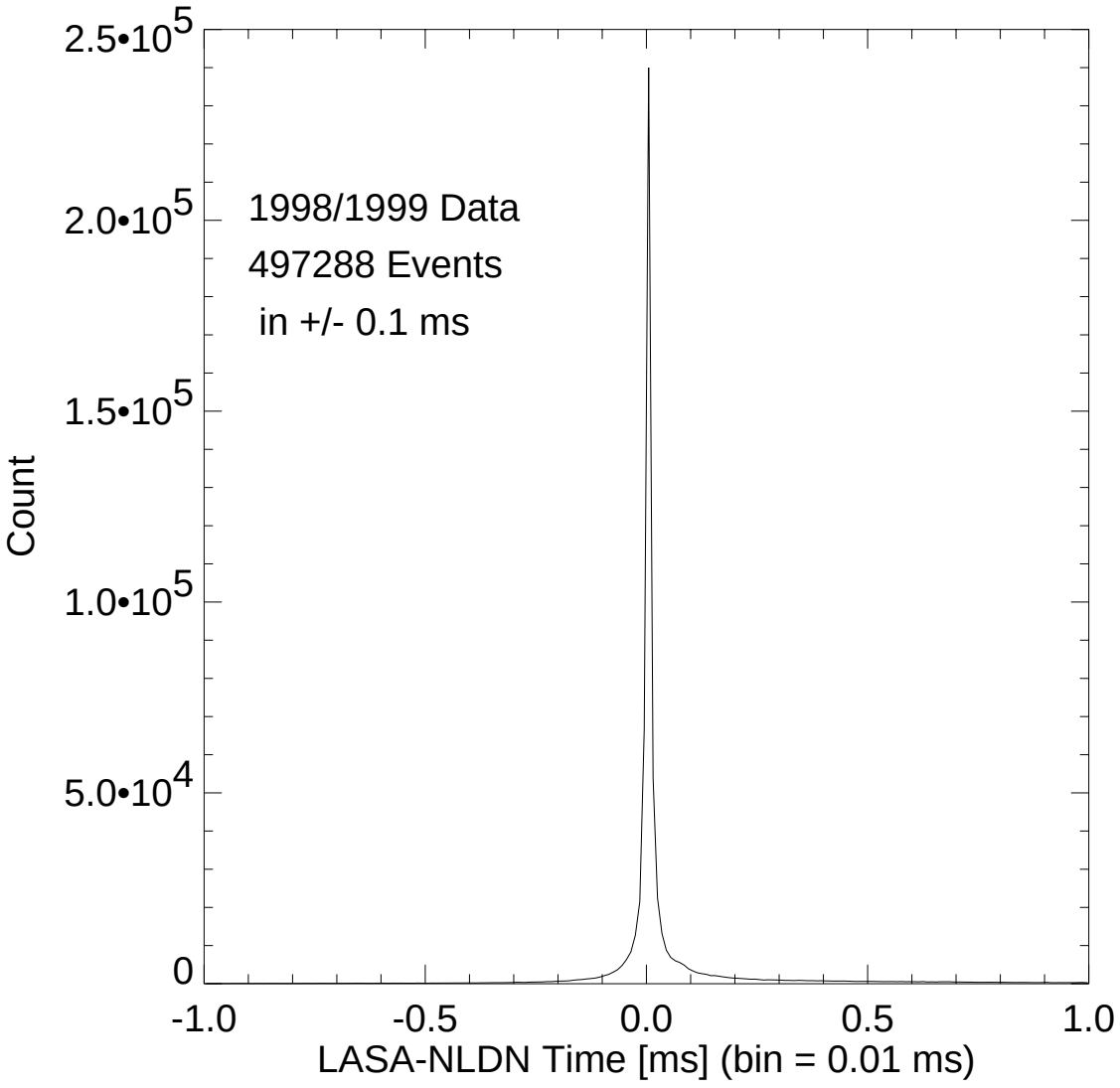

Figure 10. Histogram of LASA/NLDN time differences (1998/1999 data).

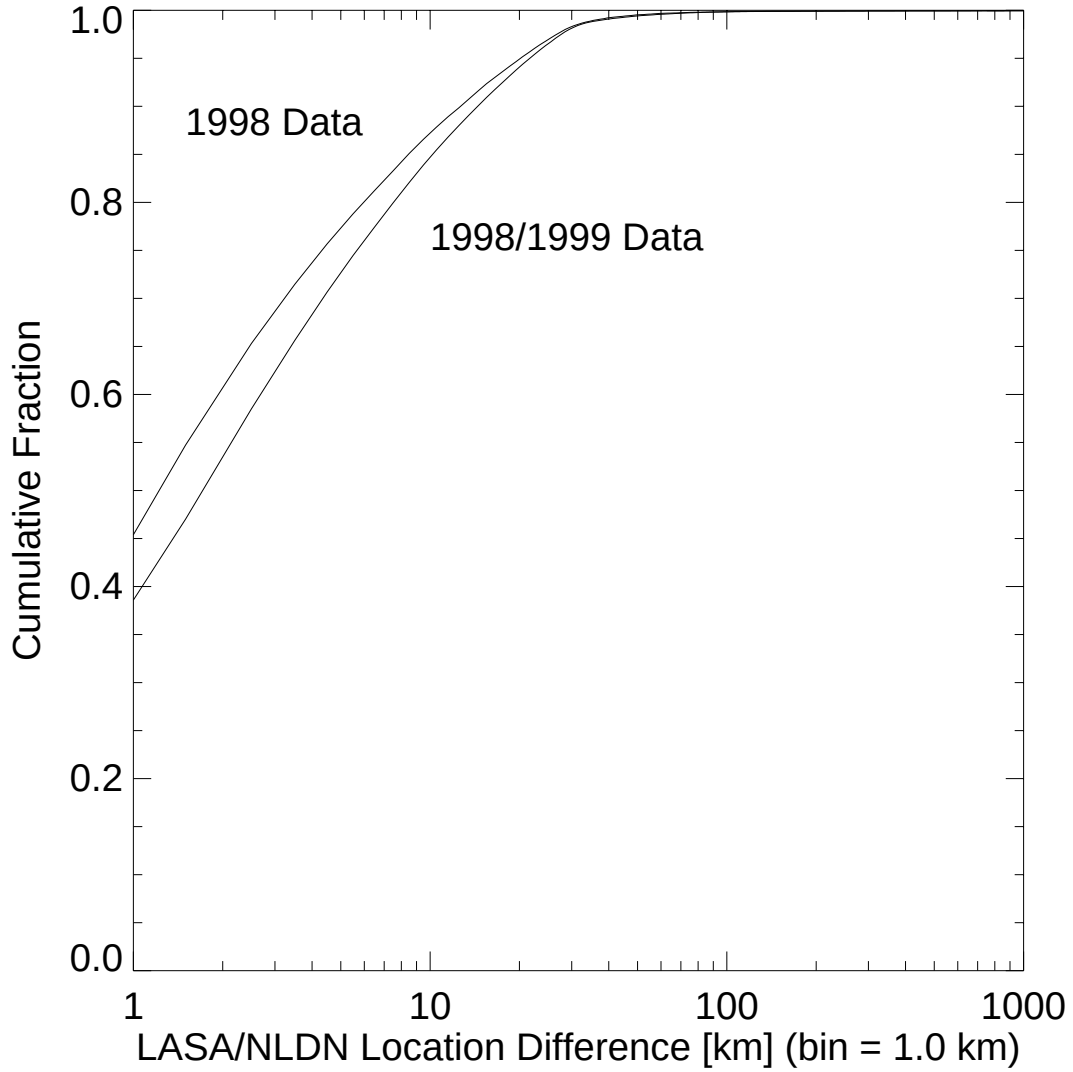

Figure 11. Cumulative log distribution of LASA/NLDN event location differences (1998 and 1998/1999 data).

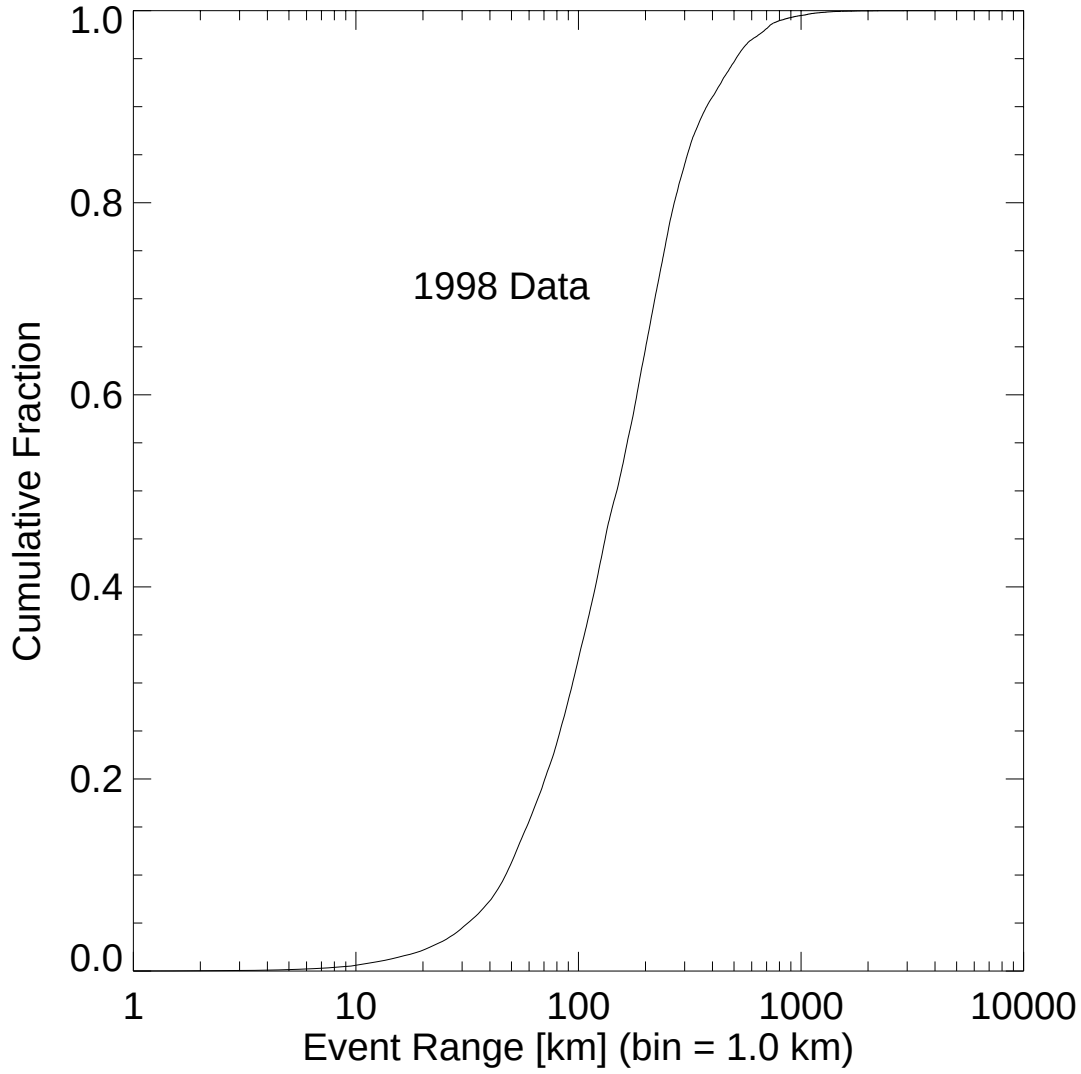

Figure 12. Cumulative log distribution of LASA event ranges from the NM array centroid (1998 data only).

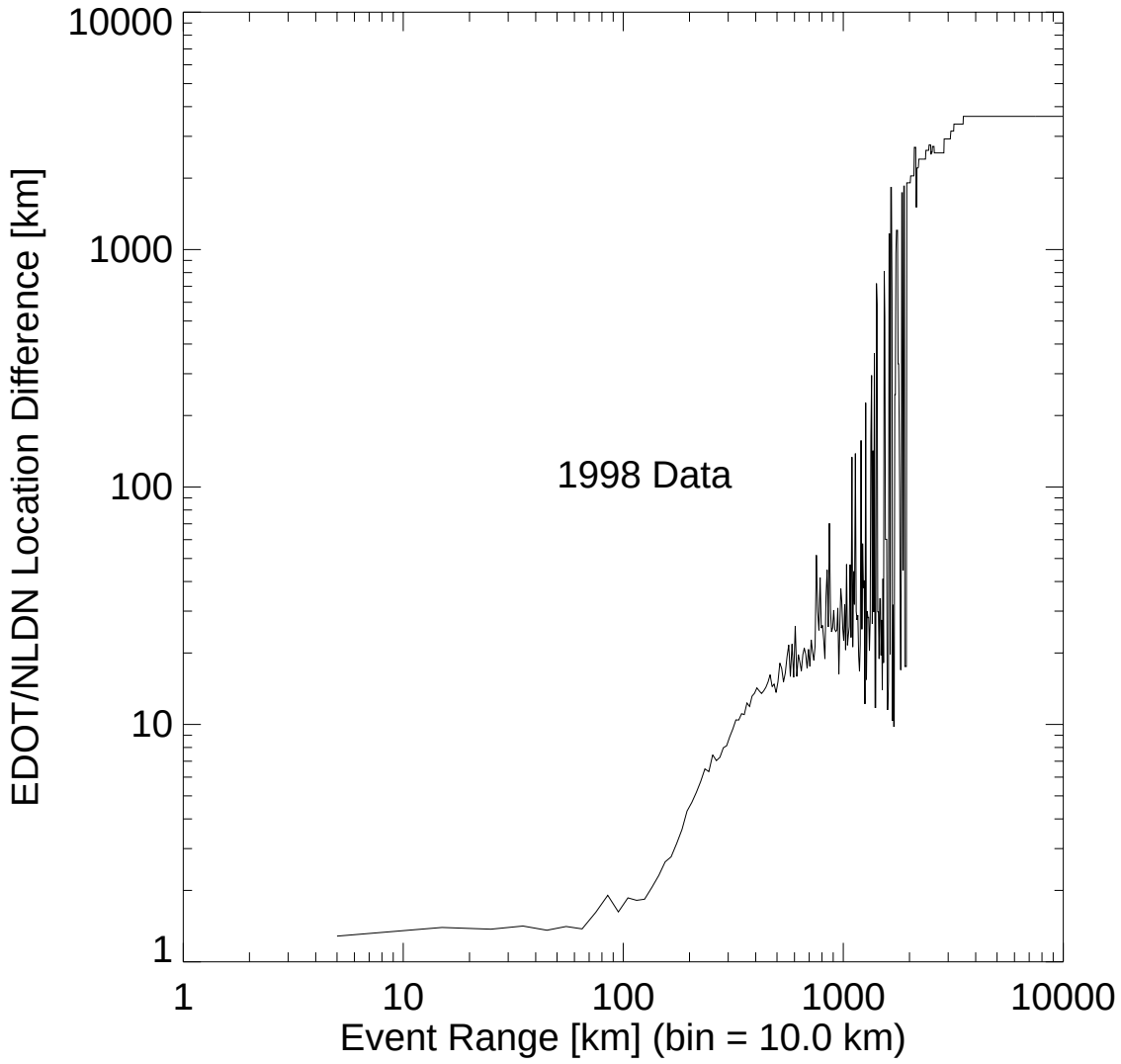

Figure 13. Log-log plot of LASA/NLDN location differences as a function of LASA event range.

4. Identification of Narrow Bipolar Pulses

Narrow bipolar electric field change pulses (NBPs) associated with very powerful RF radiation have previously been described by a number of researchers including *Le Vine* [1980], *Willett et al.* [1989], *Medelius et al.* [1991], *Smith* [1998], *Smith et al.* [1999a], and *Rison* [1999b]. *Smith et al.* [1999a] showed that the discharges occur in clouds and stated that the sources, referred to as compact intracloud discharges (CIDs), emit distinctive fast and isolated bipolar electric field change signatures. As an extension of the previous work we attempted to identify waveform qualities that would allow the events to be automatically identified in the LASA database. CIDs are excellent targets for FORTE, which regularly records RF radiation from CIDs in the form of TIPPs (transionospheric pulse pairs) [*Holden et al.*, 1995; *Massey and Holden*, 1995; *Massey et al.*, 1998].

Figures 14 and 15 show LASA examples of multiple-station narrow bipolar pulses. Figure 14 features a narrow positive bipolar pulse (NPBP) recorded by the Florida TA, GV, and BR stations on 05-30-1999 from distances of 32, 171, and 326 km respectively. The event occurred just northwest of Tampa. The pulse is so narrow on the 8 ms time scale that it is not even obvious that the initial polarity is positive. The pulses are fast and isolated with little evidence of other discharges within the waveforms. A hint of activity is visible at –1.5 ms in the TA and GV (first two) waveforms. It is highly unusual to observe signals prior to the bipolar pulses in LASA NBP field change records. Ionospheric reflections are visible in the BR (bottom) waveform within the 100 μs following the groundwave bipolar pulse. Figure 15 features a narrow negative bipolar pulse (NNBP) recorded by the New Mexico TU, RO, LA, and SO stations on 07-08-1998 from distances of 388, 544, 607, and 702 km respectively. The event occurred in Oklahoma east of the Texas Panhandle. Again the pulse is very narrow. Ionospheric reflections are visible in all three waveforms immediately following the groundwave signal.

Among the distinguishing characteristics of NBPs are their fast rise and fall times and their isolation within our 8 ms duration electric field change records. It is not unusual to see indications of subsequent IC activity in NBP field change waveforms, but it is neither common. This topic has previously been addressed by *Smith et al.* [1999a], *Smith et al.* [1999b], *Rison et al.* [1999a], and *Rison et al.* [1999b]. Figure 16 is a scatter plot of event rise-plus-fall time versus waveform signal-to-noise ratio (SNR) for the entire 1998 LASA waveform database. The determination of rise time is made by first extrapolating to zero the line that passes through the peak absolute amplitude of the waveform to the first point that exceeds ten percent of that amplitude. The rise time is the time between the zero crossing and the peak absolute amplitude. The fall time is the time between the peak amplitude and the first point to cross zero toward the opposite waveform polarity. The SNR for this study was computed by calculating the ratio of the average power within ±5 μs of the trigger point to the average power in the waveform from 6 μs after the trigger point to the end of the record. Once these parameters have been determined for each waveform that comprises an event, they are determined for the event itself. This was done by taking the average rise-plus-fall time and the minimum SNR. The minimum SNR was used rather than the average because noise in waveforms at certain stations significantly reduced NBP SNRs. The rise plus fall times in Figure 16 are in microseconds. The SNRs are in dB. Two populations are evident in the scatter plot, providing some quantitative basis for identifying CID electric field change waveforms. The minor cluster in the upper left corner of the figure represents narrow bipolar pulses, as verified by our observations of the waveforms. The large cluster of events on the lower right side of the figure includes everything else and represents the vast majority (99.3%) of events recorded during 1998. The gray line in Figure 16 was used to automatically classify events as NBPs or non-NBPs in the LASA database. Polarities of bipolar pulses were determined by assigning the polarity of the first point following the trigger point to the waveform. Table 2 shows the distribution of NNBPs, NPBPs and other events recorded in 1998 and 1999 as determined from the classification methods described in this section.

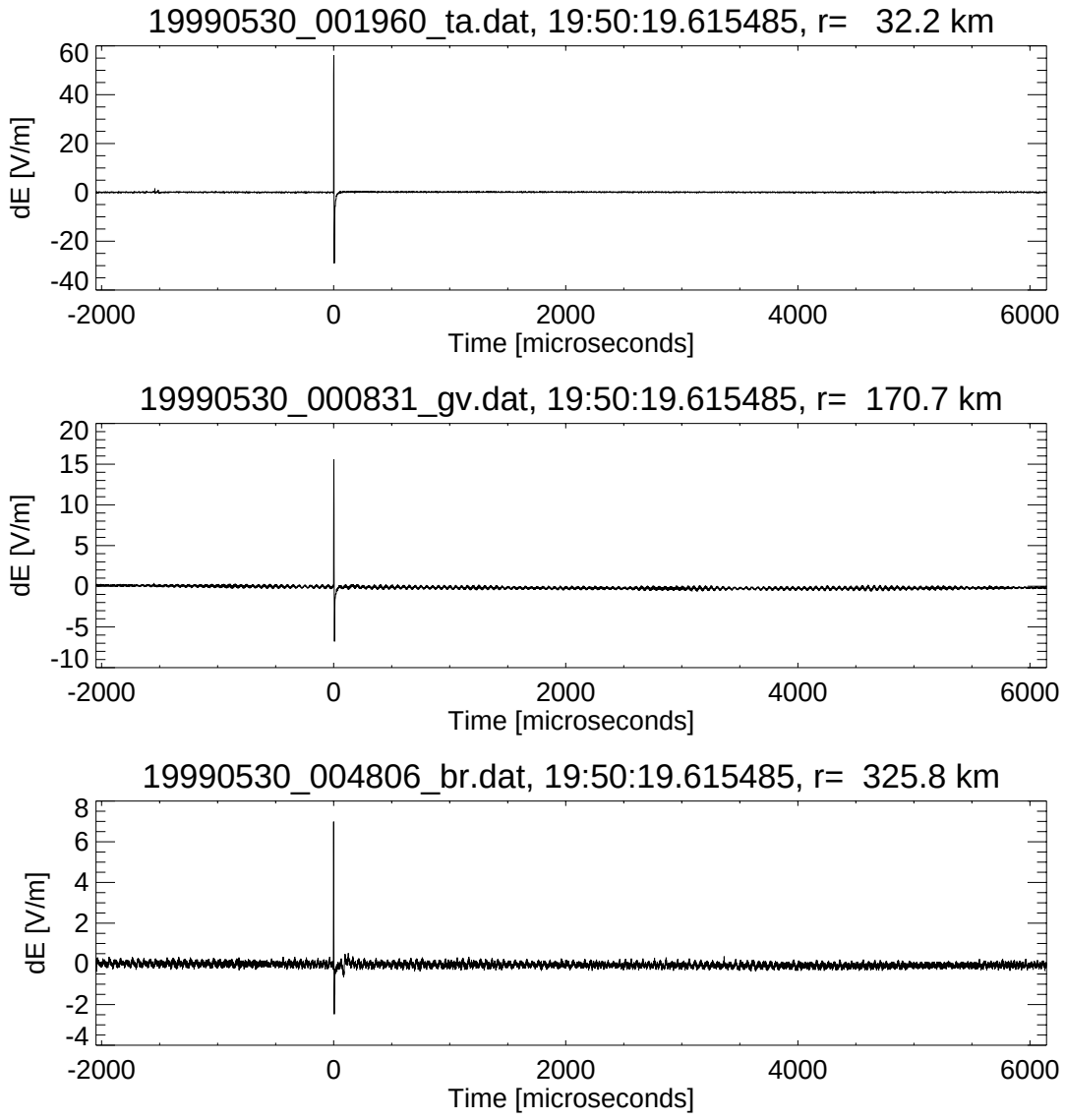

Figure 14. Narrow positive bipolar field change waveforms from a discharge that occurred 32 km northwest of Tampa.

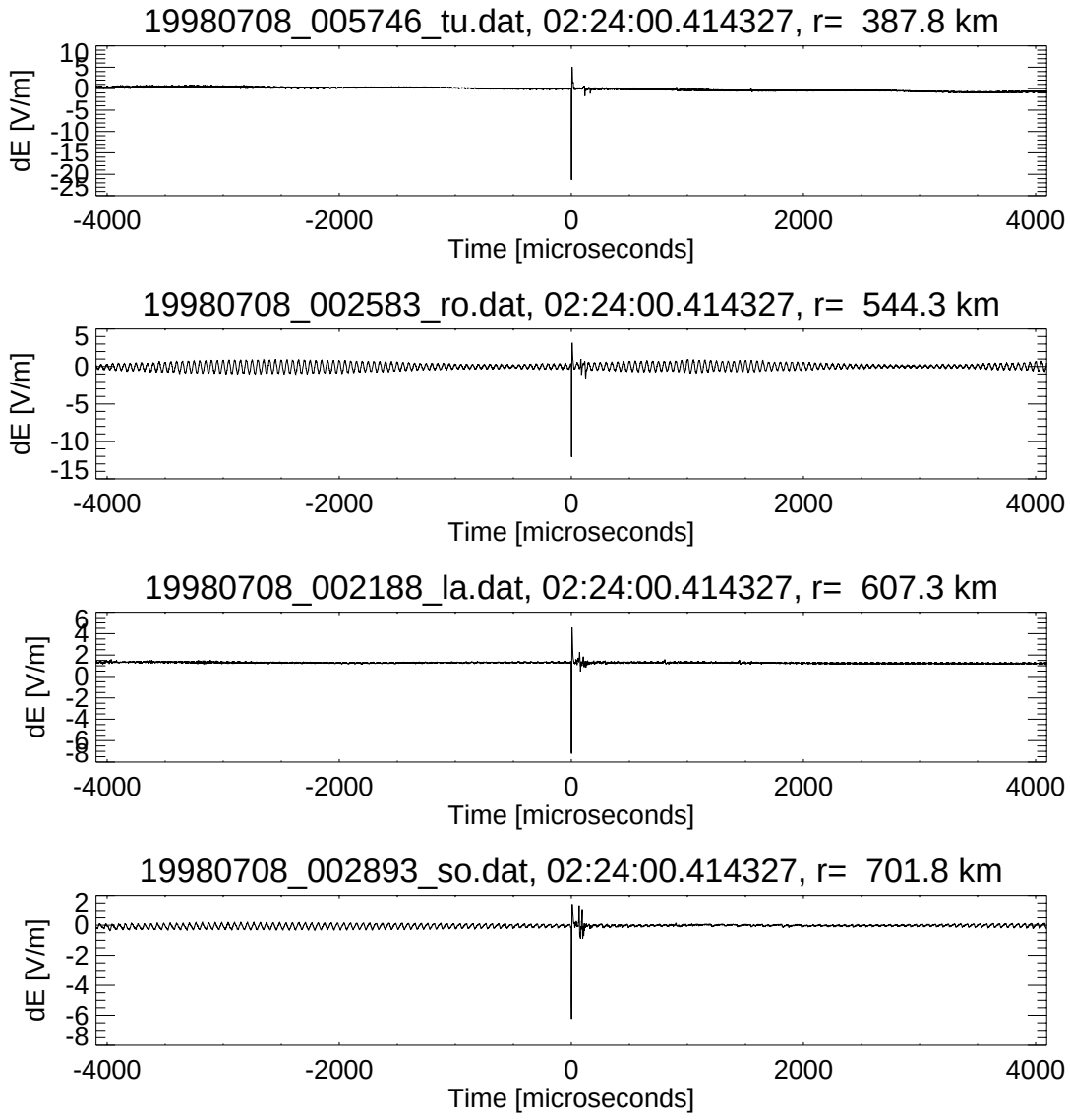

Figure 15. Narrow negative bipolar field change waveforms from a discharge that occurred east of the Texas Panhandle.

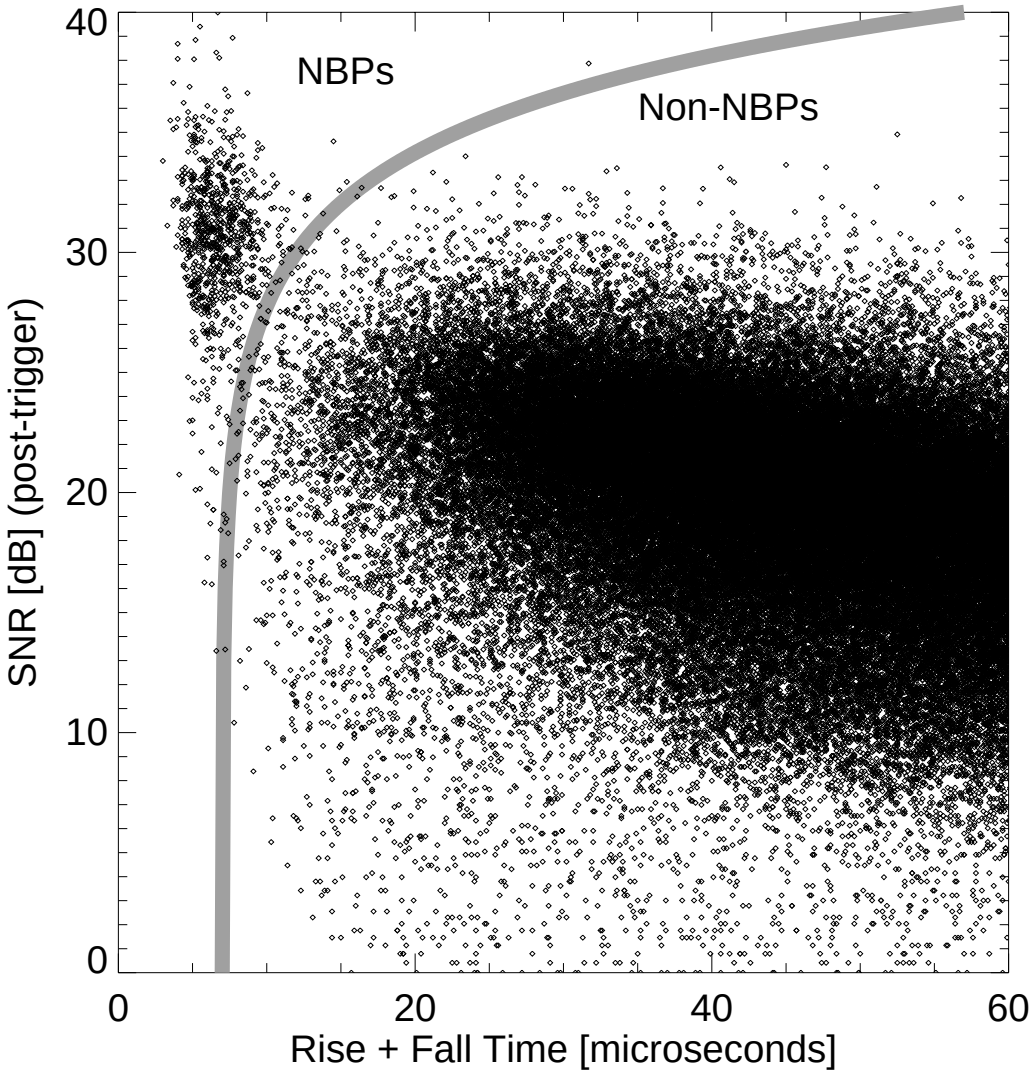

Figure 16. Scatter plot of rise-plus-fall times versus signal-to-noise ratios for all 1998 LASA events.

	1998	1999
Total Events	135,835	765,208
NPBPs	728	8462
NNBPs	134	3568

Table 2. Compilation of statistics on positive and negative narrow bipolar pulses (NBPs) in 1998 and 1999.

5. LASA-FORTE Results

The analysis of LASA/FORTE data is ongoing, but it is worthwhile to address the successfulness of joint LASA and FORTE RF observations during 1998 and 1999. As was done with the NLDN data earlier in this paper, a histogram of time differences between LASA and FORTE was formed to evaluate the significance and width of the coincidence peak. In determining event locations, LASA returns the time at which the event occurred at the determined latitude and longitude. In order to properly compare LASA time tags with FORTE it was necessary to correct for the time of flight from the LASA-determined source location to FORTE. This is because the distance from FORTE to a line-of-sight point on the ground can range from ~800 km to >3000 km, spanning a range of delays from less than three milliseconds to over ten milliseconds. Figure 17 shows a histogram of LASA/FORTE event time differences with the satellite data corrected for time of flight. The span of the histogram is ±20 ms. The bin size is 1.0 ms. A significant peak is visible near time zero with an observable noise floor of accidental coincidences. A closer look at the time differences is shown in Figure 18 where the span has been reduced to ±1.0 ms and the bin size is 50 μs. The histogram indicates that there were a couple thousand probable LASA/FORTE coincidences during 1998 and 1999. If the window is considered to be ±300 μs (a reasonable selection based on Figure 18), then the number of coincidences is 2422. Of the 2422, 101 were achieved in 1998 and 2321 in 1999.

It is interesting to consider whether campaign mode contributed to the greater yield of LASA/FORTE coincidences in 1999. A summary of the total LASA event yields compared to the number of FORTE coincidences is shown in Table 3. The data show that the likelihood of an event selected at random from the LASA database is four times as likely to have been coincident with a FORTE RF collection in 1999 as it was in 1998. This improvement is believed to be due primarily to campaign mode, which often increased LASA event detection rates by a factor of 3-5 during FORTE satellite passes and during other low-threshold time periods (as was demonstrated in Figure 4). Some of the improvement may also have been due to the expansion to Florida since, as mentioned

earlier, FORTE is able to spend more time acquiring data over the Florida than over New Mexico due to constraints involving spacecraft downlinks and uplinks with the ground stations in Albuquerque and Fairbanks.

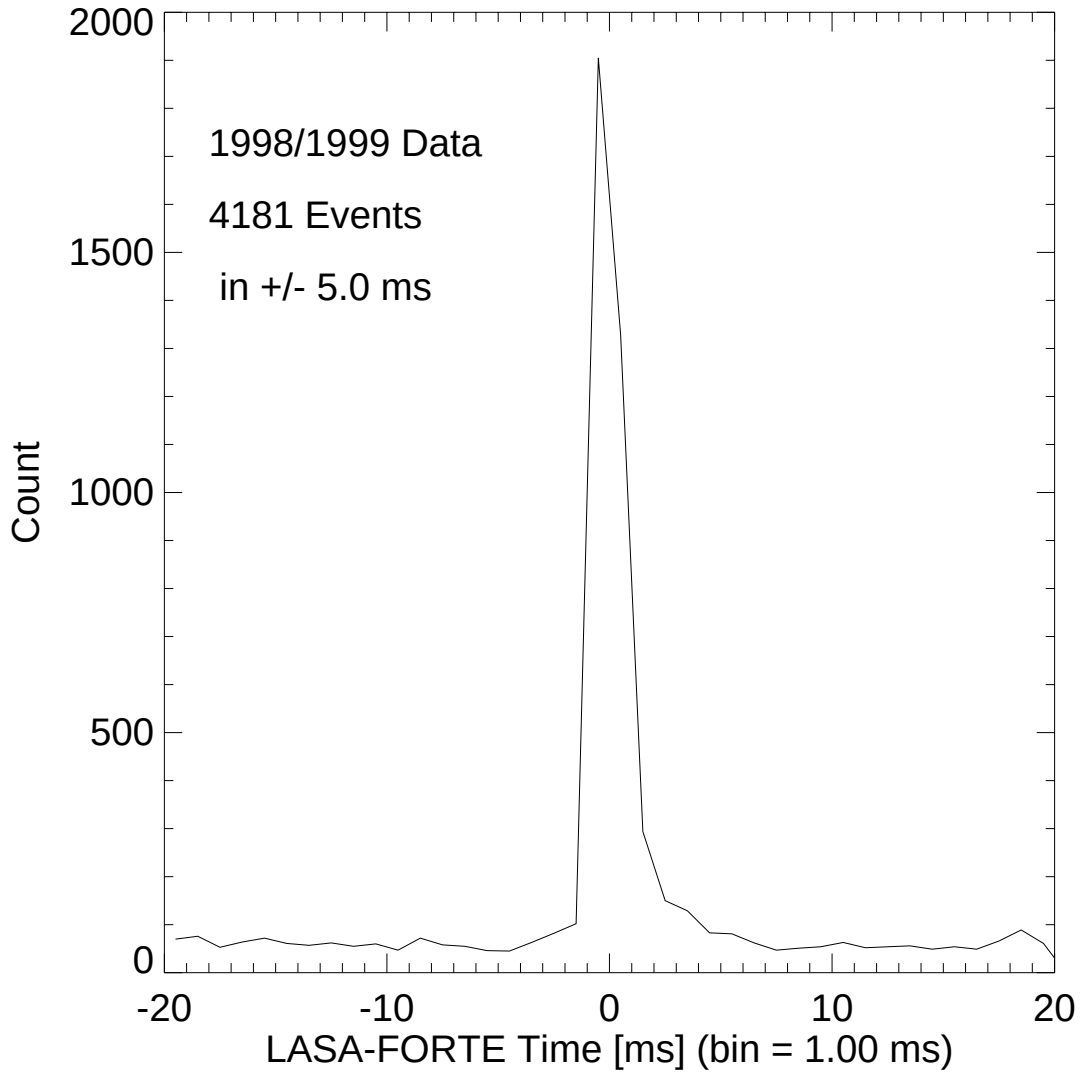

Figure 17. Histogram of LASA/FORTE time differences (1998/1999 data).

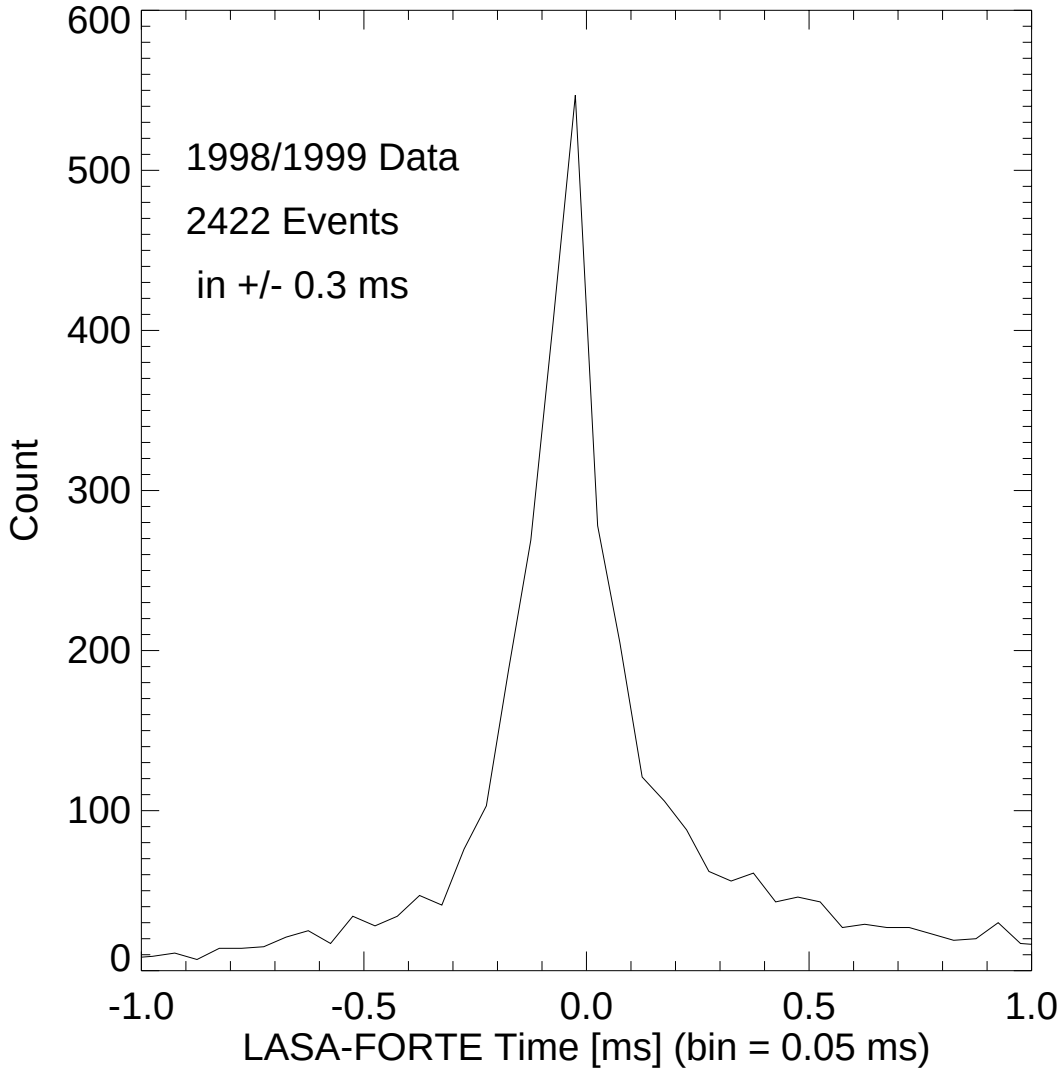

Figure 18. Histogram of LASA/FORTE time differences (1998/1999 data).

	1998	1999
Total LASA Events	135,835	765,208
FORTE Coincidences	101 (0.07%)	2321 (0.30%)

Table 3. Compilation of statistics on likelihood of LASA/FORTE coincidences in 1998 and 1999.

6. Summary

Motivation for the deployment of the Los Alamos Sferic Array was provided by the FORTE satellite project, which has a need for ground truth data that add value by providing the locations of events detected by FORTE, by further characterizing the events, or by providing background data when FORTE is not overhead. The sferic array now provides 24 hour per day lightning locations and a limited event classification capability. These data go back to May of 1998 when the array became operational. In the future the array will provide more comprehensive event classifications, as well as characterizations of event physical parameters. These expanded data sets will be applicable to the entire archive of sferic data, since all waveforms have been retained since its inception. This paper has described some of the initial location and identification capabilities as well as evaluated the successfulness of event location determination and the probability of achieving coincident detections with the FORTE satellite.

Acknowledgements

The authors wish to acknowledge the significant accomplishments of our friend and coauthor Robert (Bob) Massey, who passed away suddenly on March 5th of 1999. He was a brilliant and funny man who had a tremendous positive influence on those who knew him. He is dearly missed. Furthermore, we thank the following individuals and institutions who have hosted LANL Sferic Array stations: Tim Hamlin, Paul Krehbiel, Bill Rison, Mark Stanley, and Ron Thomas of New Mexico Tech; Richard Griego, Jesse King, Dianne Klassen, and Harold Pleasant of Eastern New Mexico University; Jim Morgan of Mesa Technical College; Dean Morss and Bob Strabley of Creighton University; Michael Brooks, John Madura, and Frank Merceret of the NASA Kennedy Space Center; Robert Chang, David Rabson, and Dale Spurgin of the University of South Florida; Walter, Leslie, and Cheryl Peterson of Cyberstreet in Fort Myers; Pat Hackett, Tom Kelly, Sal Morgera, Vichate Ungvichian, and Hank Vansant of Florida Atlantic University; Jim Goetten, Vlad Rakov, Keith Rambo, and Martin Uman of the University of Florida; and Steve Patterson and Thomas Trost of Texas Tech University. LANL personnel who also made significant contributions include Michael Carter, Diane Roussel-Dupré, Morrie Pongratz, and Marc Eberle. The enthusiastic support of all of these people made the success of this project not only possible but probable. This work was performed under the auspices of the United States Department of Energy.

References

Boccippio, D. J., S. Heckman, and S. J. Goodman, A diagnostic analysis of the Kennedy Space Center LDAR network, submitted *J. Geophys. Res.*, 2000.

Cummins, K. L., M. J. Murphy, E. A. Bardo, W. L. Hiscox, R. B. Pyle, and A. E. Pifer, A combined TOA/MDF technology upgrade of the U. S. National Lightning Detection Network, *J. Geophys. Res., 103* (D8), 9035-9044, 1998a.

Cummins, K. L., E. P. Krider, and M. D. Malone, The U. S. National Lightning Detection Network and applications of cloud-to-ground lightning data by electric power utilities, *IEEE Trans. on Electromag. Compat., 40* (4), 1998b.

Kirkland, M. W., D. M. Suszcynsky, R. Franz, J. L. L. Guillen, and J. L. Green, Observations of terrestrial lightning at optical wavelengths by the photodiode detector on the FORTE satellite, Rep. LA-UR-98-4098, Los Alamos Natl. Lab., Los Alamos, N. M., 1998.

Holden, D. N., C. P. Munson, and J. C. Devenport, Satellite observations of transionospheric pulse pairs, *Geophys. Res. Lett., 22*, 889-892, 1995.

Jacobson, A. R., S. O. Knox, R. Franz, and D. C. Enemark, FORTE observations of lightning radio-frequency signatures: Capabilities and basic results, *Radio Sci., 34* (2), 337-354, 1999.

Jacobson, A. R., K. L. Cummins, M. Carter, P. Klingner, D. Roussel-Dupré, and S. O. Knox, FORTE radio-frequency observations of lightning strokes detected by the National Lightning Detection Network, *J. Geophys. Res., 105* (D12), 15,653-15,662, 2000a.

Jacobson, A. R. and X. M. Shao, Using geomagnetic birefringence to locate sources of impulsive, terrestrial VHF signals detected by satellites on orbit, submitted *Radio Sci.*, 2000b.

Krehbiel, P. R., M. Brook, and R. A. McCrory, An analysis of the charge structure of lightning discharges to ground, *J. Geophys. Res., 84* (C5), 2432-2456, 1979.

Lee, A. C. L., Ground truth confirmation and theoretical limits of an experimental VLF arrival time difference lightning flash locating system, *Quart. J. Royal Meteorol. Soc., 115*, 1147-1166, 1989.

Light, T. E., D. M. Suszcynsky, M. W. Kirkland, and A. R. Jacobson, Simulations of lightning optical waveforms as seen through clouds by satellites, submitted *J. Geophys. Res.*, 2000.

Lennon, C., and L. Maier, Lightning mapping system, in *Proceedings of the International Aerospace and Ground Conference on Lightning and Static Electricity, NASA Conf. Publ. 3106*, pp. 89-1 to 89-10, 1991.

Le Vine, D. M., Sources of the strongest RF radiation from lightning, *J. Geophys. Res., 85*, 4091-4095, 1980.

Massey, R. S., and D. N. Holden, Phenomenology of transionospheric pulse pairs, *Radio Sci., 30*, 1645-1659, 1995.

Massey, R. S., S. O. Knox, R. C. Franz, D. N. Holden, and C. T. Rhodes, Measurements of transionospheric radio propagation parameters using the FORTE satellite*, Radio Sci., 33* (6), 1739-1753, 1998.

Massey, R. S., D. N. Holden, and X. M. Shao, Phenomenology of transionospheric pulse pairs: Further observations, *Radio Sci., 33* (6), 1755-1761, 1998.

Medelius, P. J., E. M. Thomson, and J. S. Pierce, E and DE/DT waveshapes for narrow bipolar pulses in intracloud lightning, in *Proceedings of the International Aerospace and Ground Conference on Lightning and Static Electricity, NASA Conf. Publ. 3106*, pp. 12-1 to 12-10, 1991.

Nelder, J. A. and R. Mead, *Computer Journal, 7*, p. 308, 1965.

Pinto Jr., O., I. R. C. A. Pinto, J. H. Diniz, A. M. Caravalho, and A. C. Filho, Cloud-to-ground lightning flash characteristics obtained in the southeastern Brazil using the LPATS technique and the new hybrid lightning location methodology, in *Proceedings of the 11th International Conference on Atmospheric Electricity*, edited by H. Christian, NASA/CP-1999-209261, pp. 62-64, 1999.

Press, W. H., B. P. Flannery, S. A. Teukolsky, W. T. Vetterling, Downhill simplex method in multidimensions, in *Numerical Recipes*, pp. 289-293, Cambridge University Press, Cambridge, 1986.

Proctor, D. E., A hyperbolic system for obtaining VHF radio pictures of lightning, *J. Geophys. Res., 76*, 1478-1489, 1971.

Rison, W., R. Scott, R. J. Thomas, P. R. Krehbiel, T. Hamlin, and J. Harlin, 3-Dimensional lightning and dual-polarization radar observations of thunderstorms in central New Mexico, in *Proceedings of the 11th International Conference on Atmospheric Electricity*, edited by H. Christian, NASA/CP-1999-209261, pp. 432-435, 1999a.

Rison, W., R. J. Thomas, P. R. Krehbiel, T. Hamlin, and J. Harlin, A GPS-based three-dimensional lightning mapping system: Initial observations in central New Mexico, *Geophys. Res. Lett., 26*, 3573-3576, 1999b.

Smith, D. A., Compact intracloud discharges, Ph. D. Dissertation, Dep. of Electr. Eng., Univ. of Colo., Boulder, 1998.

Smith, D. A., X. M. Shao, D. N. Holden, C. T. Rhodes, M. Brook, P. R. Krehbiel, M. Stanley, W. Rison, and R. J. Thomas, A distinct class of isolated intracloud lightning discharges and their associated radio emission, *J. Geophys. Res., 104* (D4), 4189-4212, 1999a.

Smith, D. A., R. S. Massey, K. C. Wiens, K. B. Eack, X. M. Shao, D. N. Holden, and P. E. Argo, Observations and inferred physical characteristics of compact intracloud discharges, in *Proceedings of the 11th International Conference on Atmospheric Electricity*, edited by H. Christian, NASA/CP-1999-209261, pp. 6-9, 1999b.

Suszcynsky, D. M., M. Kirkland, P. Argo, R. Franz, A. Jacobson, S. Knox, J. Guillen, J. Green, and R. Spalding, Thunderstorm and lightning studies using the FORTE optical lightning system (FORTE/OLS), in *Proceedings of the 11th International Conference on Atmospheric Electricity*, edited by H. Christian, NASA/CP-1999-209261, pp. 672-675, 1999.

Suszcynsky, D. M., M. W. Kirkland, A. R. Jacobson, R. C. Franz, S. O. Knox, J.L.L. Guillen, and J. L, Green, FORTE observations of simultaneous VHF and optical emissions from lightning: Basic phenomenology, *J. Geophys. Res., 105* (D2), 2191-2201, 2000a.

Suszcynsky, D. M., T. E. Light, S. Davis, M. W. Kirkland, J. L. Green, J. L. L. Guillen, and W. Myre, Coordinated observations of optical lightning from space using the FORTE photodiode detector and CCD imager, submitted *J. Geophys. Res.*, 2000b.

Willett, J. C., J. C. Bailey, and E. P. Krider, A class of unusual lightning electric field waveforms with very strong high-frequency radiation, *J. Geophys. Res., 94*, 16,255-16,267, 1989.